AC SAF VALIDATION REPORT

Validated products:

Name	Satellite(s)
Near real-time ozone profile Reprocessed ozone profile data record	Metop-A/B/C

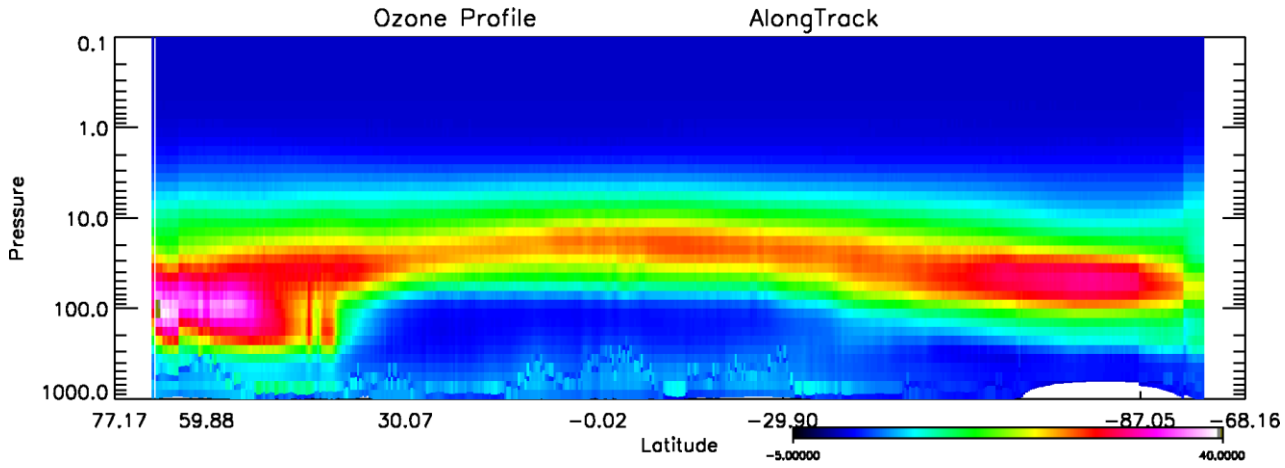

Authors:

Name	Institute
Andy Delcloo	Royal Meteorological Institute of Belgium
Katerina Garane	Aristotle University of Thessaloniki
Peggy Achtert	Deutscher Wetterdienst

Reporting period: January 2007 – August 2022

Validation methods: Lidars and microwave radiometers (altitude range 15 – 60 km)
Balloon soundings (altitude range 0 – 34 km)
Dobson and Brewer observations (total column DU)

Input data versions: GOME-2 Level 1b version 6.3.3 (01/01/2007 – 31/07/2020)
GOME-2 Level 1b version 7.0 (01/01/2007 – 31/08/2022)

Data processor versions: OPERA version 2.11

Introduction to EUMETSAT Satellite Application Facility on Atmospheric Composition monitoring (AC SAF)

Background

The monitoring of atmospheric chemistry is essential due to several human-caused changes in the atmosphere, like global warming, loss of stratospheric ozone, increasing UV radiation, and pollution. Furthermore, the monitoring is used to react to threats caused by natural hazards as well as to follow up the effects of international protocols.

Therefore, monitoring the chemical composition of the atmosphere and its effect on the Earth's radiative balance is a very important duty for EUMETSAT. The target is to provide information for policy makers, scientists and the general public.

Objectives

The main objectives of the AC SAF is to process, archive, validate and disseminate atmospheric composition products (O_3, NO_2, SO_2, BrO, HCHO, H_2O, OClO, CO, NH3), aerosol products and surface ultraviolet radiation products. The majority of the AC SAF products are based on data from the GOME-2 and IASI instruments onboard *EUMETSAT's* MetOp satellites.

Another important task besides the near real-time (NRT) and offline data dissemination is the provision of long-term, high-quality atmospheric composition products resulting from reprocessing activities.

Product categories, timeliness and dissemination

NRT products are available in less than three hours after measurement. These products are disseminated via EUMETCast, WMO GTS or the internet.

- Near real-time trace gas column (total and tropospheric O_3 and NO_2, total SO_2, total HCHO, CO) and high-resolution ozone profile
- Near real-time absorbing aerosol index (AAI) from main science channels and polarization measurement detectors
- Near real-time UV index, clear-sky and cloud-corrected

Offline products are available within two weeks after measurement and disseminated via dedicated web services at EUMETSAT and AC SAF.

- Offline trace gas column (total and tropospheric O_3 and NO_2, total SO_2, total BrO, total HCHO, total H_2O) and high-resolution ozone profile
- Offline absorbing aerosol index from main science channels and polarization measurement detectors
- Offline surface UV, daily doses and daily maximum values with several weighting functions

Data records are available after reprocessing activities from the EUMETSAT Data Centre and/or the AC SAF archives.

- Data records generated in reprocessing
- Lambertian-equivalent reflectivity
- Total OClO

Users can access the AC SAF offline products and data records free of charge by registering at the AC SAF web site.

More information about the AC SAF project, products and services: https://acsaf.org/

AC SAF Helpdesk: helpdesk@acsaf.org

Bluesky: https://bsky.app/profile/ac-saf.eumetsat.int

Applicable AC SAF Documents

[ATBD] Algorithm Theoretical Basis Document for Near Real Time and Offline Ozone profiles, KNMI/GOME/ATBD/01/001, issue 2.1.3, Olaf Tuinder, November 2022.

[PUM] Product User Manual for Near Real Time and Offline Ozone profiles, KNMI/GOME/PUM/001, issue 2.5.2, Olaf Tuinder, November 2022.

Both documents are available at http://acsaf.org in the *Documents* section.

Table of Contents

Acronyms and abbreviations

ATBD	Algorithm Theoretical Basis Document
AUTH	Aristotle University of Thessaloniki
DOAS	Differential Optical Absorption Spectroscopy
GAW	Global Atmosphere Watch
GDP	GOME Data Processor
GOME	Global Ozone Monitoring Experiment
LAP/AUTH	Laboratory of Atmospheric Physics/Aristotle University of Thessaloniki
MetOp	Meteorological Operational satellite
MWR	Microwave Radiometers
NDACC	Network for the Detection of Atmospheric Composition Change
NH	Northern Hemisphere
O3-CCI	Ozone – Climate Change Initiative
OMI	Ozone Monitoring Instrument
OPERA	Ozone Profile Retrieval Algorithm
SH	Southern Hemisphere
SZA	Solar Zenith Angle
TOC	Total Ozone Column
TOMS	Total Ozone Mapping Spectrometer
TrOC	Tropospheric integrated Ozone Column
WMO	World Meteorological Organization
WOUDC	World Ozone and UV Data Center

General Introduction

This report contains validation results of the GOME-2/MetOpB and GOME-2/MetOpC data (hereafter GOME-2A, GOME-2B and GOME-2C) integrated ozone profiles were retrieved by the algorithm and using the methodology that is described in the "NRT, Offline and Data Record Vertical Ozone Profile and Tropospheric Ozone Column Producs" ATBD (Tuinder, 2022). The GOME-2 integrated ozone profile datasets used in this validation report cover the following time periods:

- GOME-2A: 4 January 2007 – 15 November 2021
- GOME-2B: 29 October 2012 – 31 August 2022
- GOME-2C: 3 January 2019 – 31 August 2022

The datasets were provided by the KNMI algorithm team in the form of overpass files for a specified number of ground-based stations.

Ozone profiles retrieved from reprocessed level-1b data were retrieved with 80 km x 40 km horizontal resolution.

Since this work was carried out in three different institutions, this document is split up into three separate parts. The first part contains the validation of the retrieved GOME-2 ozone profiles using ozonesondes (chapter 2). This part validates the retrieved ozone profiles in the troposphere and the lower stratosphere. The second part (chapter 3) uses measurements with lidars and microwave radiometers to assess the performance of GOME-2 ozone profiles; primarily in the stratosphere from 20 to 60 km altitude. The third part of this report (chapter 4), covers the validation of the integrated ozone profile product through an intercomparison with ground truth data from spectrophotometers (Dobson and Brewer). Additionally, the consistency of the integrated ozone profiles from GOME-2A/2B/2C are examined by intercomparison to the respective products from GOME-2A/2B/2C, as well as the official TOC products of GOME-2A/2B/2C, processed with the GDP4.9 algorithm. This work is done by AUTH. The outcome of the different validation parts is summarized in the summary and conclusions section at the end of this report. Table 1.1 presents the different accuracies which are taken into account to assess the quality of the product.

Table 1.1: Different intended accuracies for ozone profiles, provided in the Product Requirements Document SAF/AC/FMI/RQ/PRD/001

Accuracy		
Threshold	**Target**	**Optimal**
30 % in stratosphere	15 % in stratosphere	10 % in stratosphere
70 % in troposphere	30 % in troposphere	25 % in troposphere

1. Validation of ozone profiles using ozonesondes

1.1 *Introduction*

This report presents validation results for the AC SAF GOME-2A/2B/2C reprocessed ozone profile products. The validation was carried out using ozone sounding profiles.

Ozonesondes are lightweight balloon-borne instruments which measure ozone concentrations from the surface up to about 30 km with much better vertical resolution than possible from satellite data. In general, measurement precision and accuracy are also better compared to satellite observations, at least in the lower stratosphere and the troposphere. Another advantage is that ozone soundings can be performed at any time and during any meteorological condition.

The precision of ozonesondes varies with altitude and depends on the type of ozonesonde used. **Error! Reference source not found.** shows indicative precision of the Electrochemical C oncentration Cell (ECC) and Brewer-Mast (B-M) ozonesondes at different pressure levels of the sounding.

Table 1.1: Precision (in percent) of different types of ozonesondes at different pressure levels.

Pressure level (hPa)	ECC	B-M
10	2	10
40	2	4
100	4	6
400	6	16
900	7	14

Profiles from ozonesondes are most reliable around the 40 hPa level, which is around the ozone maximum. The error bar of profiles from ozonesondes increases rapidly at levels above the 10 hPa level, which is at around 31 km altitude. For this validation report, only the station of Hohenpeissenberg is using B-M sondes. The other stations under consideration (**Error! R eference source not found.**) use ECC sondes.

1.2 *Dataset description*

GOME-2A/2B/2C ozone data used in this validation report covers the time periods mentioned in section the general introduction:

- GOME-2A: 4 January 2007 – 15 November 2021
- GOME-2B: 29 October 2012 – 31 August 2022
- GOME-2C: 3 January 2019 – 31 August 2022

GOME-2A/2B/2C ozone data was made available by KNMI at pre-selected site where ozone soundings are performed on a regular basis. Data was made available by the World Ozone and Ultraviolet Data Center (WOUDC). (http://www.woudc.org) and the NILU's Atmospheric Database for Interactive Retrieval (NADIR) at Norsk Institutt for Luftforskning (NILU) (http://www.nilu.no/nadir/). In Figure 1.1, Figure 1.1: Stations consulted for validation. Latitude belts from north to south: polar stations north: green (67N – 90 N), midlatitude stations north: black (30 N – 67 N), Tropical stations: red (30 N – 30 S), midlatitude stations south: grey (30 S – 70 S), polar stations south: blue (70 S – 90 S). An overview is shown from the ozonesonde station data used in this report.

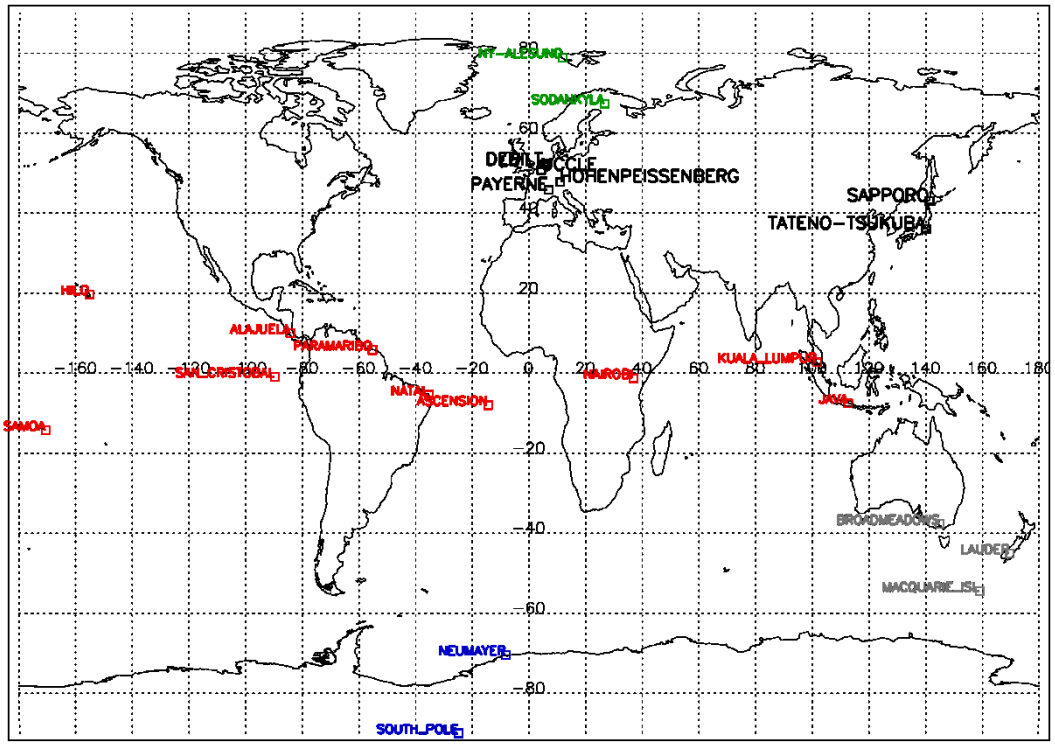

Figure 1.1: Stations consulted for validation. Latitude belts from north to south: polar stations north: green (67N – 90 N), midlatitude stations north: black (30 N – 67 N), Tropical stations: red (30 N – 30 S), midlatitude stations south: grey (30 S – 70 S), polar stations south: blue (70 S – 90 S).

1.3 *Comparison procedure*

1.3.1 Co-location criteria

The selection criteria are twofold:

- The geographic distance between the GOME-2 pixel center and the sounding station location is less than 100 km.
- The time difference between the pixel sensing time and the sounding launch time is less than ten hours.

Each sounding that is correlated with a GOME-2 overpass is generally correlated with several GOME-2 pixels if the orbit falls within this 100 km circle around the sounding station. This means that a single ozone profile is compared to more than one GOME-2 measurement.

1.4 *Ozone sounding pre-processing*

GOME-2 ozone profiles are given as partial ozone columns on 40 varying pressure levels calculated by the Ozone Profile Retrieval Algorithm (OPERA) developed by KNMI. Ozone partial columns are expressed in Dobson Units.

Ozonesondes measure ozone concentration along the ascent with a typical vertical resolution of 100 m while GOME-2 profiles consist 40 layers between the ground and 0.001 hPa. Ozonesondes give ozone concentration in partial pressure. The integration requires interpolation, as GOME-2 levels never match exactly ozonesonde layers. This interpolation causes negligible errors given the high vertical resolution of ozonesonde profiles.

For comparison, ozonesonde profiles are integrated between the GOME-2 pressure levels. When a single ozonesonde profile is compared to different GOME-2 profiles, the actual reference ozone values are not the same given that the GOME-2 level boundaries vary from one measurement to another. Integrated ozonesondes data will be referred to in this report as X_{sonde}.

GOME-2 layers are relatively thick and GOME-2 layer boundaries show small variations compared to the layer thickness. Hence, individual layers generally occur around the same altitude. The altitude of those layers can be considered as "fixed" and therefore the center of an "*averaged layer altitude (or pressure)*" is used in plotting the data.

In this report, the validation of the GOME-2 profiles is calculated by using the averaging kernels (AVK) of the GOME-2 profile. The motivation to apply the AVK is to "smooth" the ozone soundings towards the resolution of the satellite:

$$X_{avk\_sonde} = X_{apriori} + A\,(X_{raw\ sonde} - X_{apriori}) \qquad (1)$$

Where A represents the averaging kernel, X_{avk_sonde} is the retrieved ozone sonde profile, X_{sonde} is the ozone sonde profile and $X_{apriori}$ is the a priori profile.

1.5 *Results*

1.5.1 Difference profiles

The relative difference between the ozone profiles from GOME-2 and an ozonesonde is calculated as:

$$(X_{GOME\text{-}2} - X_{sonde})/X_{sonde.} \quad (2)$$

For comparing the GOME-2 ozone profile with the smoothed ozonesonde profiles (AVK ozonesondes) the following equation is used:

$$(X_{GOME\text{-}2} - X_{AVK\text{-}SONDE})/X_{AVK\text{-}SONDE} \quad (3)$$

Figure 1.1 shows relative difference profiles between GOME-2 ozone profiles at the one hand and on the other hand ozonesonde-, and AVK ozonesonde profiles for different latitude belts and using different types of ozonesondes, listed inTable 1.1.

For the polar and midlatitude stations, the difference plots in Figure 1.1 show that GOME-2 ozone profiles are within the target error range of 15% compared to the ozonesonde reference, except for the Upper Troposphere – Low Stratosphere (UTLS) region. For the lower troposphere, most of the latitude belts show relative differences within 15%. Applying the averaging kernels improves the comparison significantly. For the tropical stations, there is a significant overestimation of tropospheric ozone, but the statistics are within the threshold value of 50%.

These results show that the statistics for the new GOME-2C ozone profile product compared to GOME-2B and GOME-2A show similar behaviour, with in general obtaining better results for the new sensor GOME-2C which are closer to the target values (Tab) for the different height ranges under consideration.

Since tropospheric integrated ozone column (TrOC) is an official operational product, its results are not mentioned in this report. Here we will focus on the quality of the ozone profiles and the way we communicate the results in the two-yearly operational reports. These documents are available at http://acsaf.fmi.org in the *Documents* section (operational reports).

Table 1.1 provides an overview of the height ranges related to the troposphere, the UTLS-zone and the stratosphere.

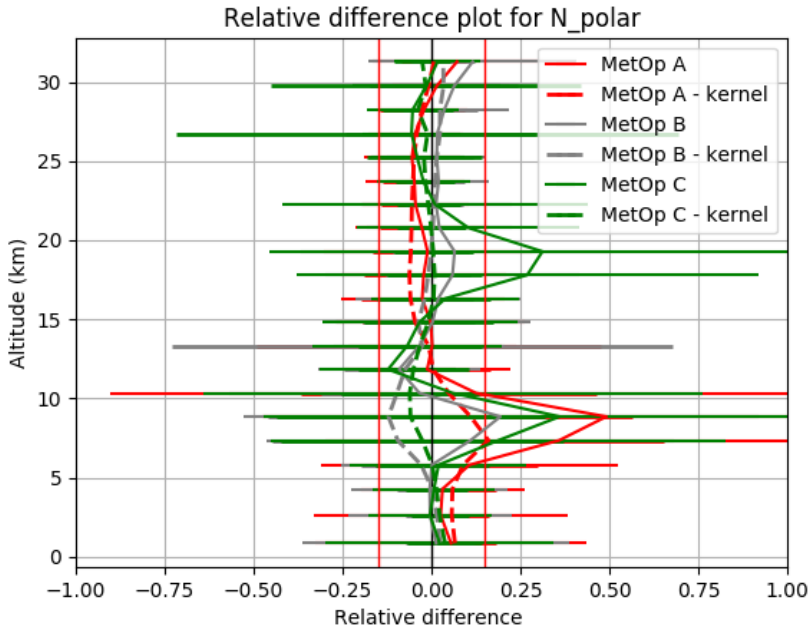
Relative difference plot for N_polar
MetOp A
MetOp A - kernel
MetOp B
MetOp B - kernel
MetOp C
MetOp C - kernel
Altitude (km)
Relative difference

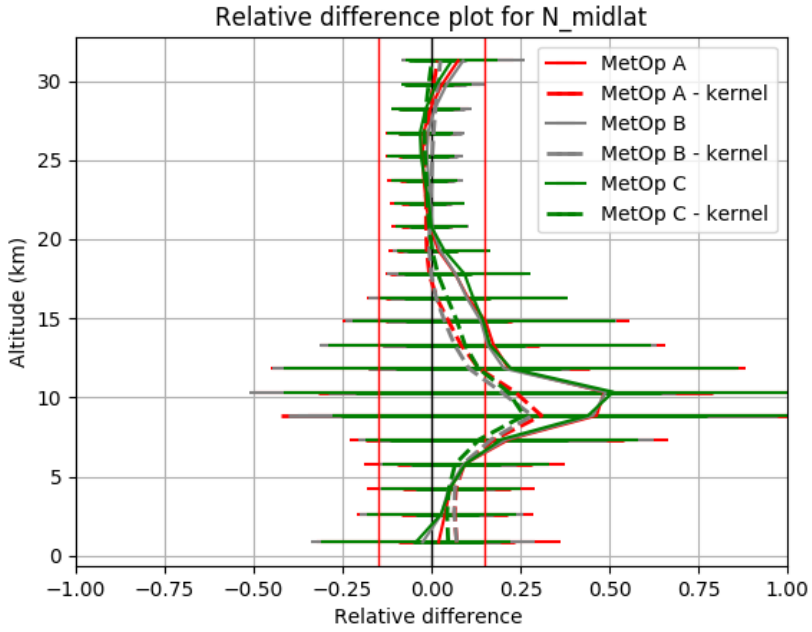
Relative difference plot for N_midlat
MetOp A
MetOp A - kernel
MetOp B
MetOp B - kernel
MetOp C
MetOp C - kernel
Altitude (km)
Relative difference

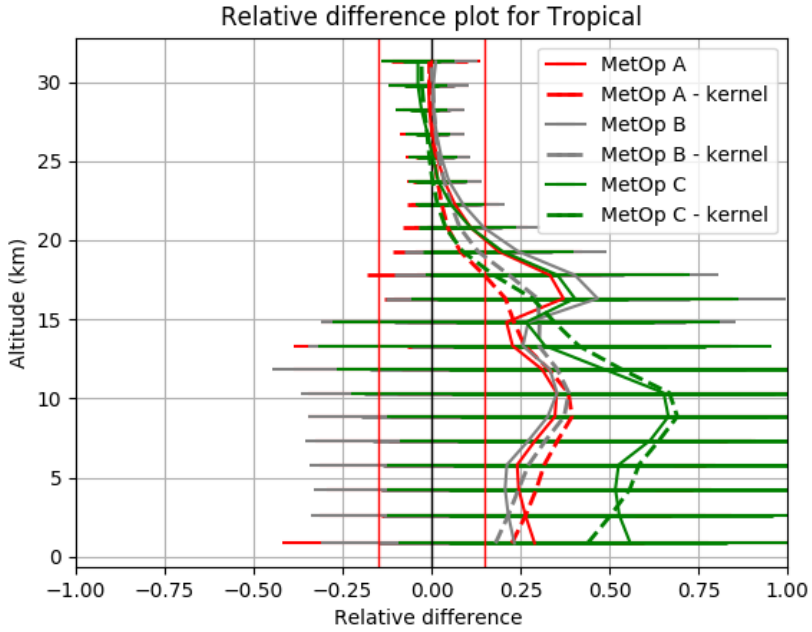
Relative difference plot for Tropical
MetOp A
MetOp A - kernel
MetOp B
MetOp B - kernel
MetOp C
MetOp C - kernel
Altitude (km)
Relative difference

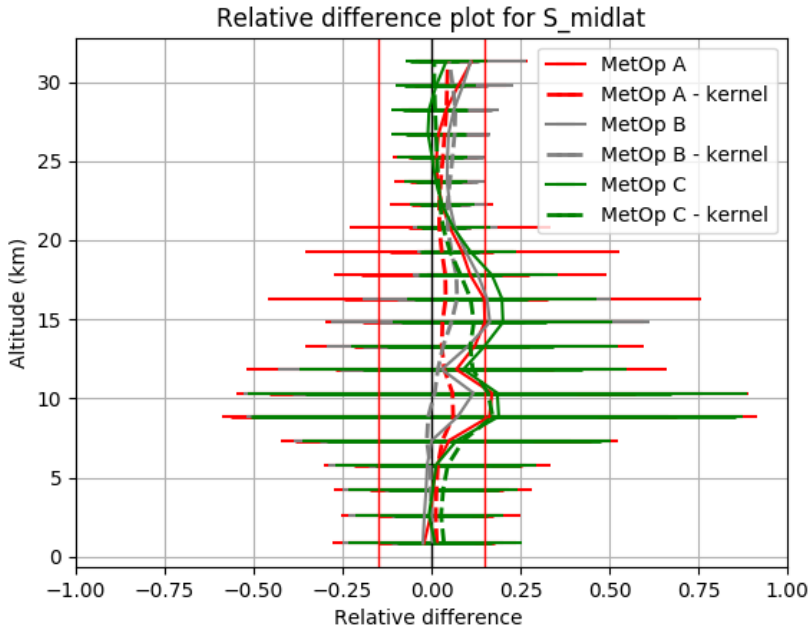
Relative difference plot for S_midlat
MetOp A
MetOp A - kernel
MetOp B
MetOp B - kernel
MetOp C
MetOp C - kernel
Altitude (km)
Relative difference

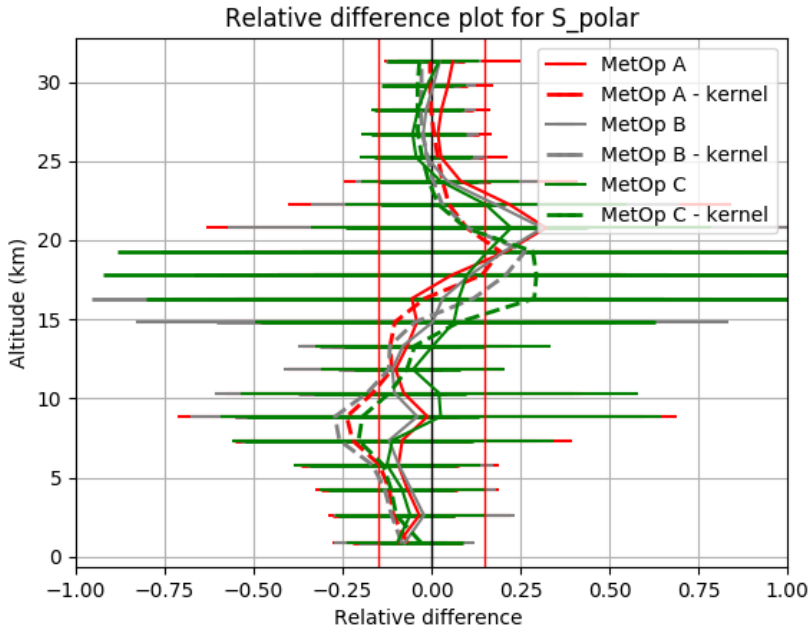

Figure 1.1: Relative difference in ozone profiles from GOME-2, ozonesondes and smoothed ozonesondes according to equations (2) and (3) for different latitude belts and for different sensors (GOME-2A/2B/2C) for the time periods as mentioned in Dataset description. The error bars represent one standard deviation on the mean error.

Table 1.1: Definition of the ranges in km for troposphere, UTLS-zone and stratosphere for the different latitude belts.

	Troposphere	UTLS	Stratosphere
Polar Regions	< 6 km	6 km - 12 km	12 km - 30 km
Mid-Latitudes	< 8 km	8 km - 14 km	14 km - 30 km
Tropical Regions	< 12 km	12 km - 18 km	18 km - 30 km

The results for the lower stratosphere are shown in ***Table 2.3: Absolute Differences (AD), Relative Differences (RD) and standard deviation (STDEV) of GOME-2A HR ozone profile products versus ground-based reference profiles for lower and upper stratosphere and different latitude belts. Results are for the time period January 2007 to December2018. The upper table is for HR data and the lower for the reprocessed data. Please note that the statistics include FTIR measurements compared to previous reports. Table 2.3***. This Table shows that for the ozone profile product, also the optimal values are met in the lower stratosphere. This is not taking into account the UTLS-zone, which shows more elevated relative differences that cannot be appointed to the troposphere or the stratosphere. This report shows the results on the ozone profile product, including lower

stratosphere and higher stratosphere. Results for the troposphere are shown in the validation report on tropospheric ozone column products, available at https://acsaf.org in the documents section (validation reports).

1.6 *Solar Zenith Angle dependency*

Previous studies with GOME-2/MetOp-A data (Delcloo and Kreger, 2013) have shown that the GOME-2 ozone profile retrieval shows a seasonal dependency and is also influenced by the Solar Zenith Angle (SZA). Figure 1.2 and Figure 1.3 show the dependency on SZA for the northern midlatitude and the northern polar stations for GOME-2B. Especially for the high ozone concentrations around 22-23 km in altitude (location of the ozone maximum), a seasonal behavior is present.

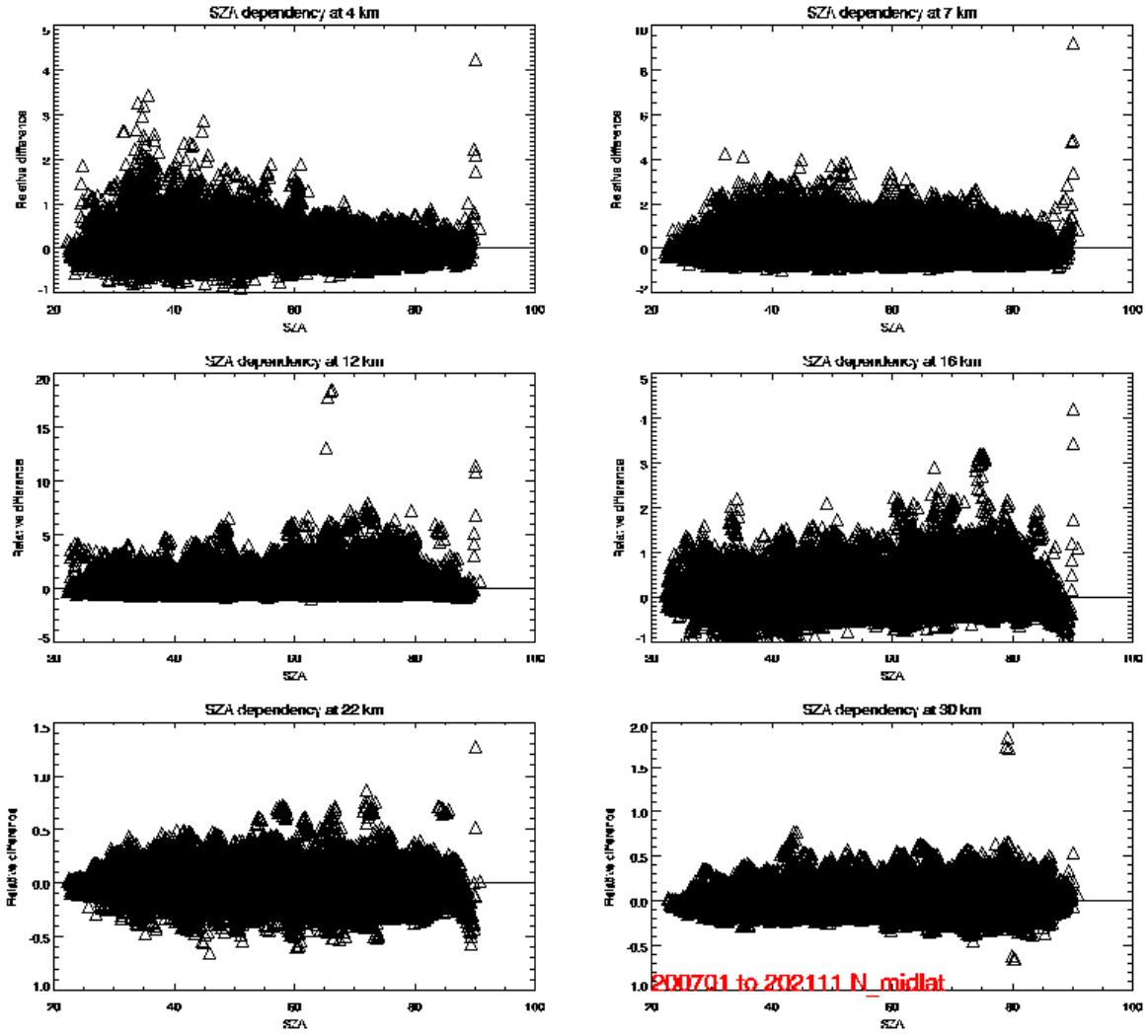

Figure 1.2: Solar Zenith Angle dependency at six altitude levels for the northern midlatitude stations for the reprocessed GOME-2A dataset.

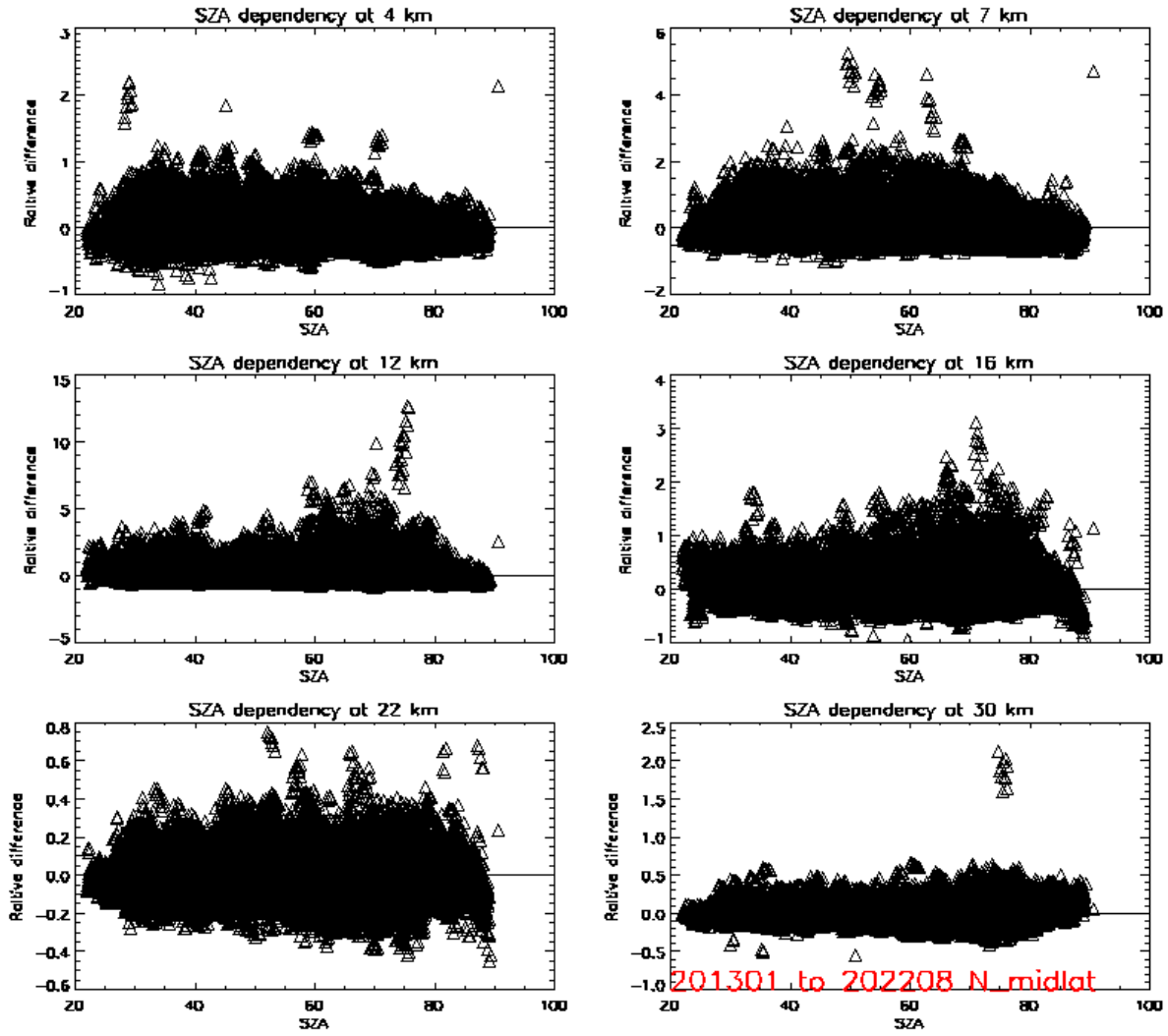

Figure 1.3: Solar Zenith Angle dependency for six altitude levels for the northern midlatitude stations for the reprocessed GOME-2B dataset

1.7 *Information content*

Scatter plots, showing the retrieved ozone partial columns as a function of the reference partial column measured by ozonesondes give a measure of the amount of information actually present in the retrieved layer. This is shown in Figure 1.4 for the northern midlatitude stations at six different altitude levels. The slope of the regression line can be seen as a measure for the amount of information actually present in the retrieved layer. To show the influence of applying the averaging kernels it is shown from Figure 1.5 that the slope values are improved (closer to 1) while the intercept values are closer to 0.

The interpretation of "better results" should be taken with care. Applying the kernels using equation 1 is a way to smooth the ozone profile towards a comparable vertical resolution of the

retrieved ozone profile. High resolution effects like filaments present for example in secondary ozone maxima are mostly not seen by GOME-2 which results in sometimes large differences between observed and retrieved partial ozone columns.

The regression line in the scatter plots show that GOME-2 loses sensitivity in the lower troposphere and around the UTLS-zone (Figure 1.4).

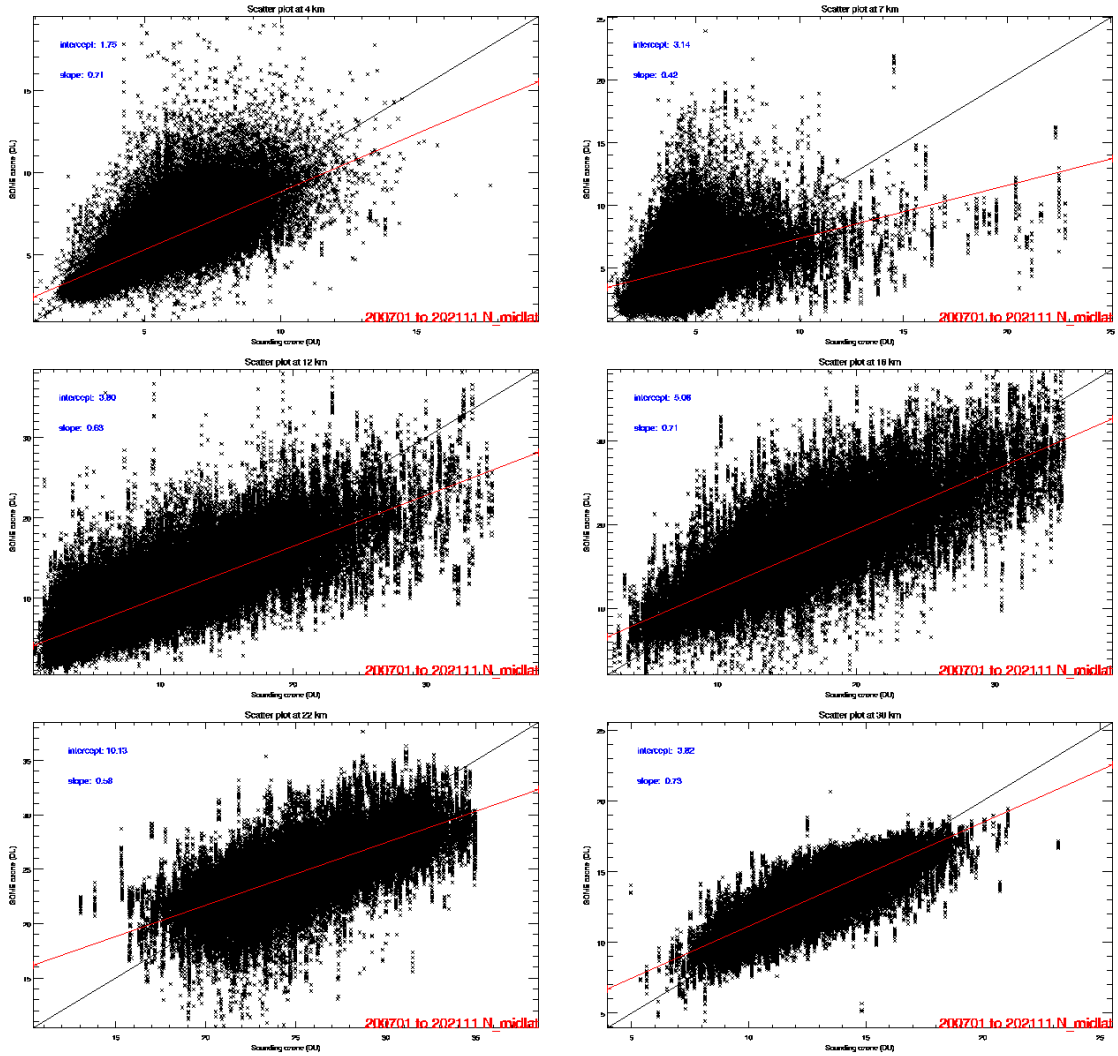

Figure 1.4: Scatter plot at 6 different altitude levels for the stations at northern midlatitudes for the reprocessed GOME-2A dataset

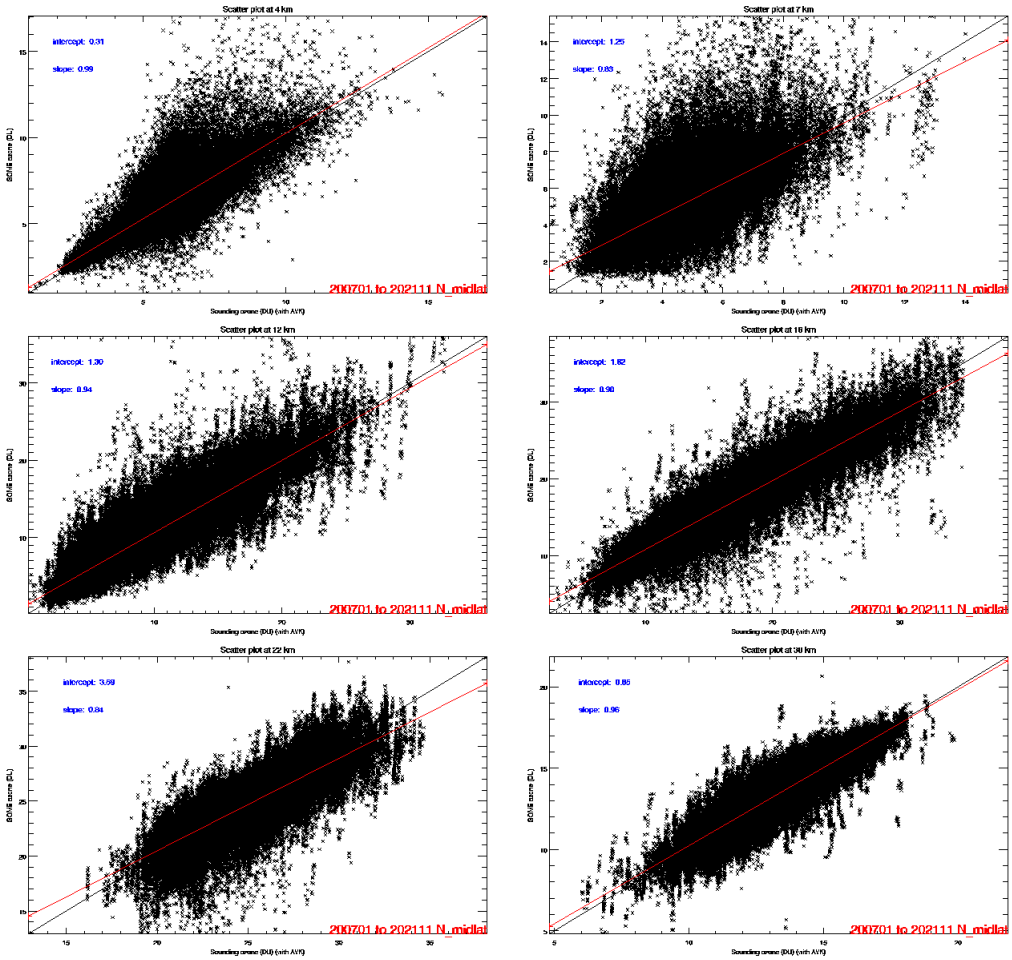

Figure 1.5: Scatter plot at 6 different altitude levels for the stations at northern midlatitudes for the reprocessed GOME-2A dataset, applying the kernels

Besides the influence on SZA, the dependence on cloud cover, seasonal behaviour has been verified. For cloud cover, we could not pinpoint any specific dependence on cloud cover. For the seasonal behaviour, it is known from previous reports (Delcloo and Kreher, 2013) that there is some seasonal behaviour present. This is especially true for the lower altitudes and can be seen in the Figure 1.8 for northern midlatitude stations. More results can be consulted on the official validation website for ozone profiles: when this product is declared operational.

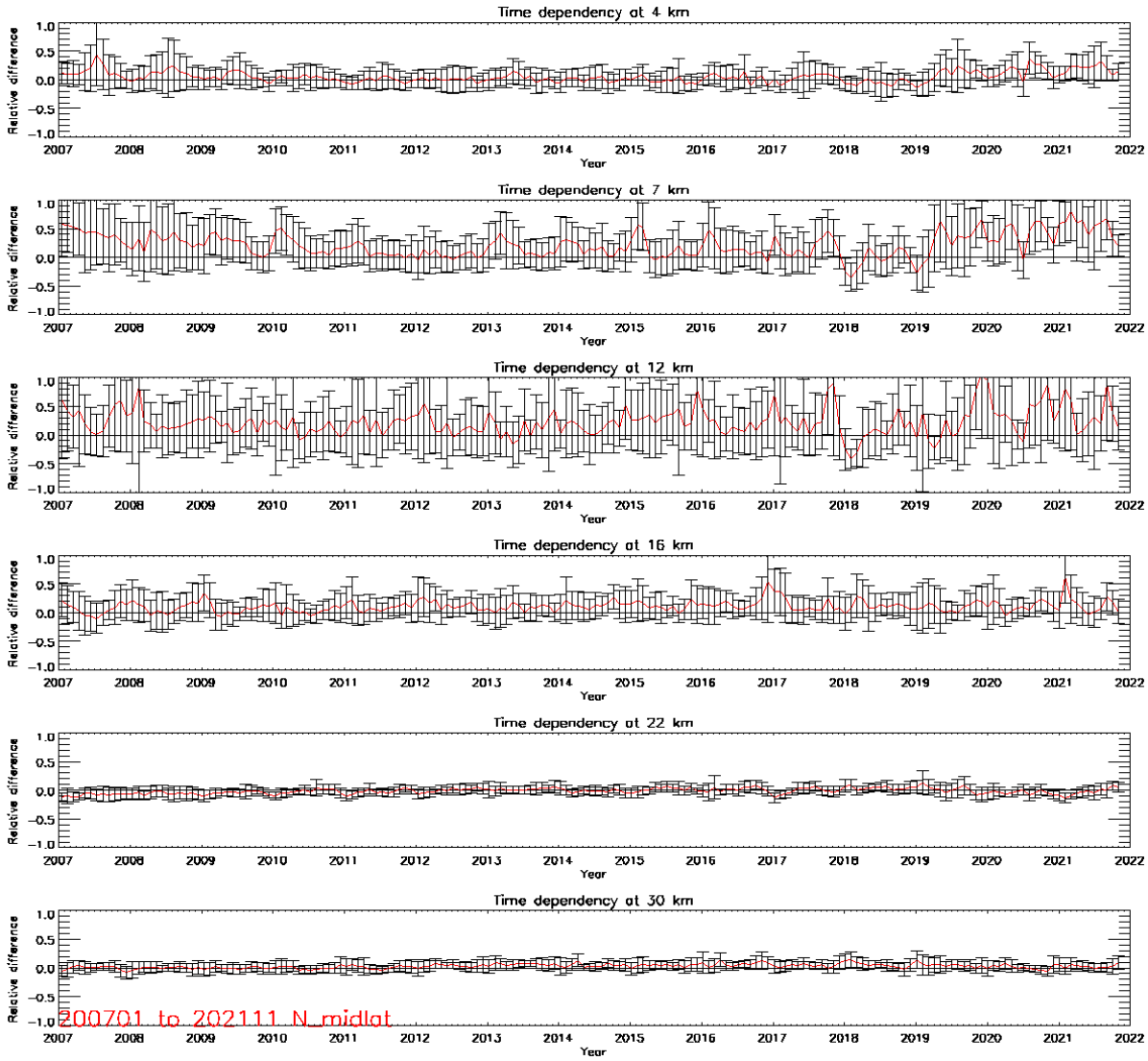

Figure 1.6: Time series at 6 different altitude levels for the stations at northern midlatitudes, GOME-2A (January 2007 – November 2021)

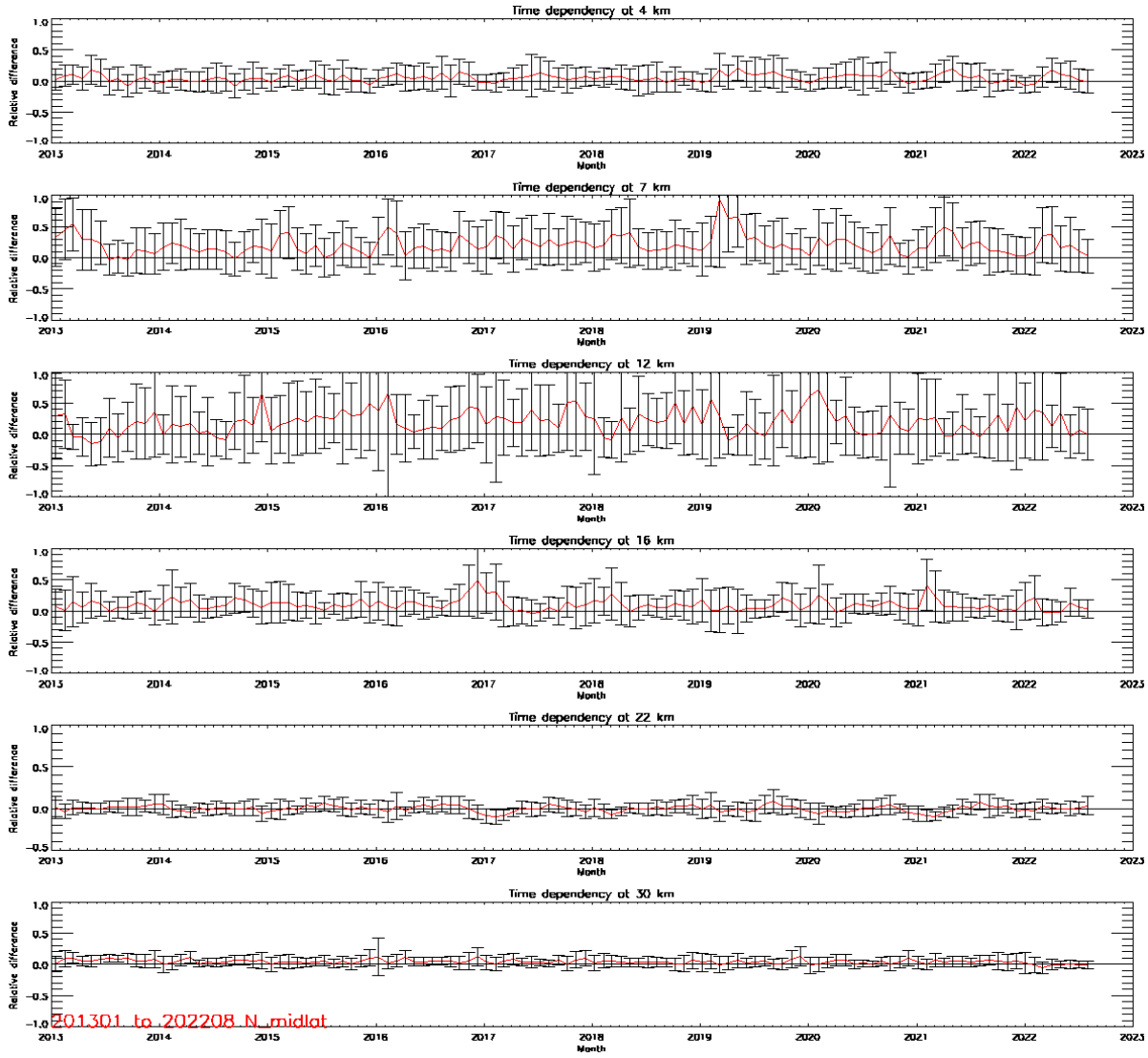

Figure 1.7: Time series at 6 different altitude levels for the stations at northern midlatitudes, GOME-2A (January 2013 – August 2022)

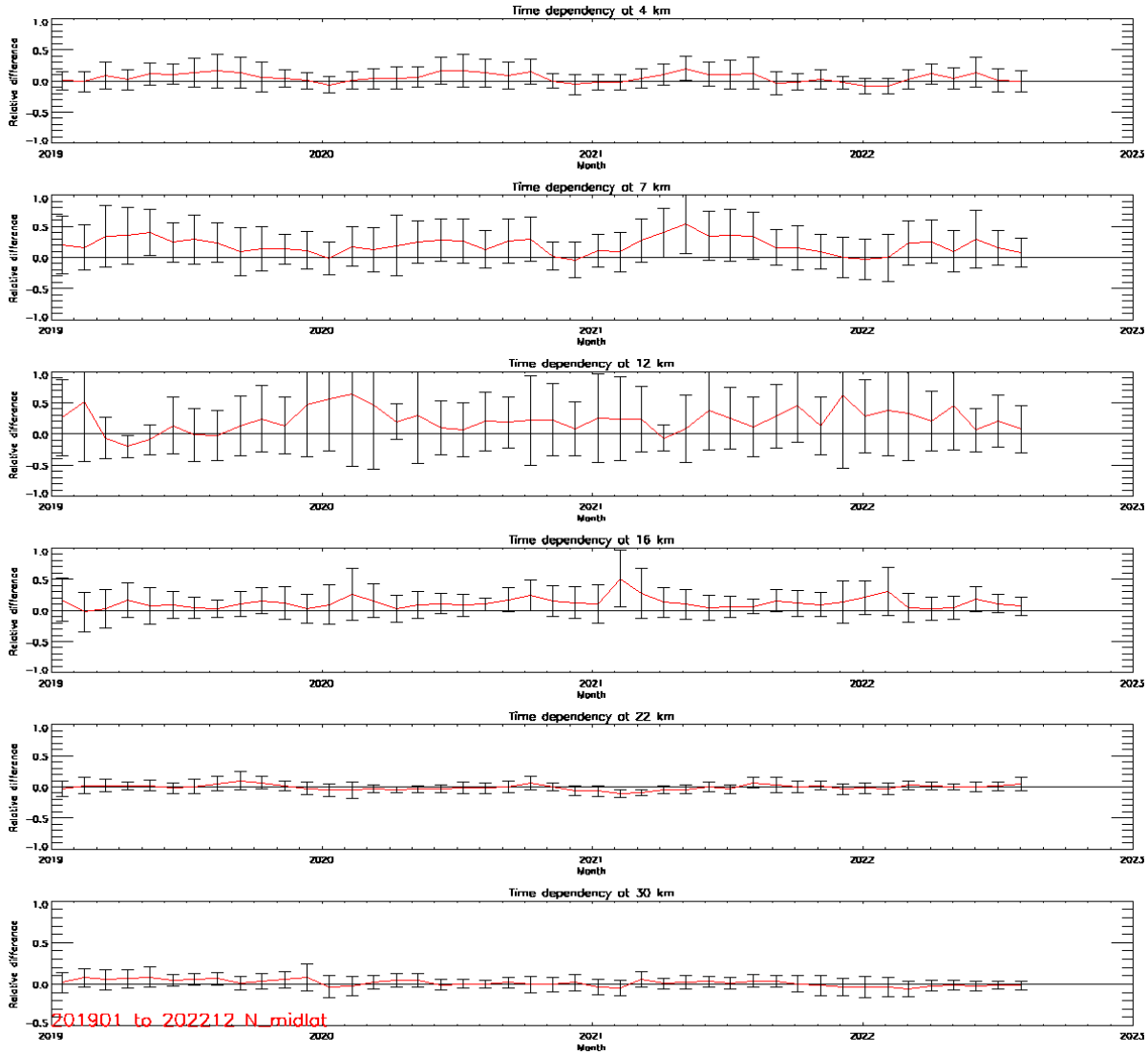

Figure 1.8: Time series at 6 different altitude levels for the stations at northern midlatitudes, GOME-2C (January 2019 – August 2022)

1.8 *General conclusions for the validation of ozone profiles, using ozonesondes*

The GOME-2A/2B/2C vertical ozone profile products were validated using ozonesonde data. The validation results have revealed the following properties:

- The comparisons of all three sensors show comparable results and are all within target value for the lower stratosphere.
- GOME-2 ozone profile retrieval shows a Solar Zenith Angle (SZA) dependency, especially for the altitude range 20 – 25 km (region where the ozone maximum is located).
- Besides the influence on SZA, the dependency on cloud cover and seasonal behaviour has been verified. For cloud cover, we could not pinpoint any specific dependency. For the seasonal behaviour, this dependency is true for the lower altitudes of the ozone profile.

It is shown that the optimal value (10% accuracy) is met in the lower stratosphere (Table 2.3) for all belts under consideration.

2. Stratospheric ozone profiles validation of reprocessed ozone profiles with lidar, FTIR and microwave instruments

2.1 *Instruments*

Lidars, fourier transform infrared (FTIR) spectrometry and microwave radiometers (MWR) are the main ground-based instruments available for validation purposes in the upper stratosphere. Their altitude range covers typically 15 km to 50 or 60 km (Table 2.1). This significantly extends the range covered by ozonesondes towards higher altitudes. It also provides a good overlap from 15 to 30 km altitude. Note that there are only about five long term operational lidar, nine FTIR and four MWR stations on the globe that provide regular data, though not as rapidly and operationally as the ozonesonde stations. Typically, ozone profiles do not become available until several weeks after the measurement.

The Differential Absorption Lidar (DIAL) technique provides accurate vertical profiles of ozone in the altitude range from 15 to 50 km, depending on the individual lidar system (Godin et al., 1989). Clouds and daylight conditions inhibit good measurements (Leblanc and McDermid, 2000; Steinbrecht et al., 2006), so lidar ozone profiles are restricted to cloud free nights. Typically, 5 to 8 lidar measurements per month are taken at a station. Depending on atmospheric conditions and lidar system efficiency, each ozone profile measurement covers several hours. For the lidars, number density versus geometric altitude is the natural coordinate system of the measurement.

An FTIR spectrometer measures ozone profiles between 3 and 42 km by analysing the interaction of infrared radiation with the atmosphere. The instrument records high-resolution infrared spectra. Ozone absorbs certain wavelengths of infrared light due to its molecular

structure. The FTIR spectrometer detects this absorption and converts the information into an ozone spectrum using the Fourier transform method. This conversion allows ozone concentration to be represented as a function of altitude. The total error range is from 1.5 to 2.5 % between 250 and 3000 DU (Garcia et al. 2022) without a simultaneous temperature fit, but around 1.5% when a temperature retrieval is included in the data retrieval.

MWR measures the thermal radiation of a pressure broadened emission line. Line-shape depends on the pressure/altitude profile of ozone (Lobsiger et al., 1984; Parrish et al., 1988). Measurement of the precise line-shape, thus, allows for retrieving the ozone profile. Similar to many satellite measurements, an optimal estimation retrieval (Rodgers, 1990) provides ozone profiles in various coordinate systems, including number density versus altitude for the NDACC MWR profiles. MWR ozone profiles typically cover 20 to 60 km altitude. In contrast to lidars, MWR has little weather dependence, and measures during daylight as well. On average, MWR profiles are measured on 20 days per month. The integration time of one MWR profile varies from 30 minutes to 5 hours, depending on the individual instrument (Boyd et al., 2007; Hocke et al., 2007).

Table 2.1: Typical precision and height resolution of lidars and MWR (Steinbrecht et al., 2006)

	Lidar		microwave radiometer	
Height [km]	**Precision [%]**	**height resolution [km]**	**precision [%]**	**height resolution [km]**
15	5	1.4		
20	5	1.2	3	10
25	3	1.0	3	10
30	3	1.8	3	10
35	3	4.2	3	14
40	5	7.2	3	14
45	15	8.6	3	20
50	55	8.6	3	20
50-70			3	20

2.2 *Dataset description*

The ground-based validation profiles come from the NDACC (Network for the Detection of Atmospheric Composition Change, http://www.ndsc.ncep.noaa.gov/). NDACC lidar and microwave instruments go through an evaluation process and thorough quality checks (Keckhut et al., 2004). The ozone profiles are not available in near real time. A minimum of one month

is necessary before profiles become available but most stations need three or more months. NDACC demands that ozone profiles are submitted at least once per year to their database.

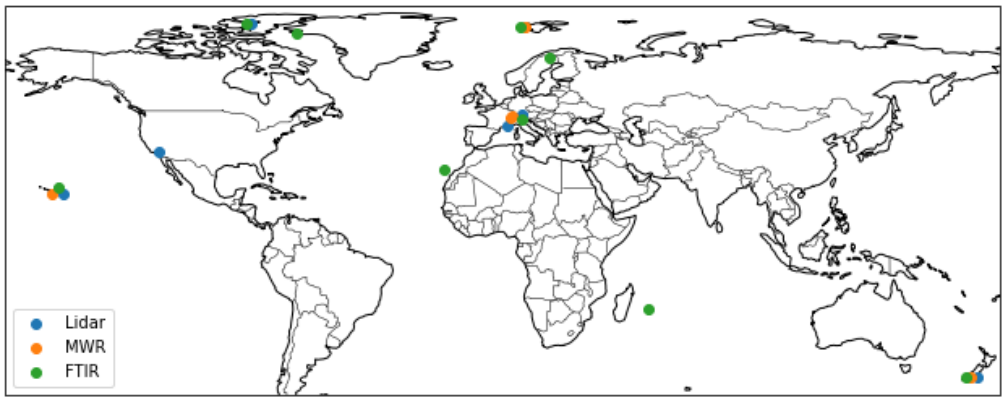

Figure 2.1: Stations consulted for validation. Lidar station in blue, FTIR in green and microwave radiometer station in orange.

The stations (***Figure 2.1***, Table A.4) used in this validation for the lidar/microwave data are from the Network for the Detection of Atmospheric Composition Change (NDACC): Ny-Ålesund (microwave, FTIR), Payerne (microwave), Hohenpeissenberg (lidar, FTIR at Zugspitze), Bern (microwave), Haute-Provence (lidar), Table Mountain (lidar), Mauna Loa (lidar, FTIR and microwave), Izana (FTIR), Reunion-Maido (FTIR), Eureka (FTIR), Kiruna (FTIR), Thule (FTIR), and Lauder (lidar and FTIR). Polar stations north is located between 65N and 90 N, the mid-latitude stations north is between 25° N and 65° N, and the tropical stations are located between 25° N and 25° S.

2.3 *Comparison procedure*

Generally, the comparison procedure is the same as for the ozonesondes, outlined in Section 1 (see also Delcloo and Kins, 2009; 2012). Different temporal resolution and measurement frequency of the ground-based instruments, however, require some minor changes.

2.4 Co-location criteria in time and space

Only ground-based and satellite profiles that are close in space and in time to a GOME-2 profile are compared. Nightly mean lidar measurements are compared to GOME-2 profiles measured either the morning after or the morning before the lidar profile. This means that a maximum time difference of 20 hours is allowed.

MWR measure around the clock, typically one profile every hour. So usually, MWR profiles can be compared with GOME-2 ozone profiles measured within less than 2 hours. Usually all GOME-2 measurements are made in the local morning.

FTIR measurements are compared with GOME-2 ozone profiles measured within less than 2 hours.

Only GOME-2 profiles with ground pixels canters closer than 200 km to the validation stations are considered. A 200 km radius typically gives about 50 co-located GOME-2 high-resolution

profiles per station and per day. The number of coarse resolution profiles is lower, but still provides a good statistical basis. Larger co-location radii result in larger geophysical differences, smaller radii result in too few comparisons cases.

2.5 Pre-processing of the ground-based ozone profiles.

Like the ozonesonde data, lidar, FTIR and MWR ozone number density profiles are first averaged over the GOME-2 retrieval layers, usually 40 layers, about 2 km wide. The resulting slightly smoothed profiles are called $X_{ref.}$

In the next step, the X_{ref} lidar, FTIR and MWR profiles are further smoothed over altitude by applying the GOME-2 averaging kernels (with proper scaling). These smoothed profiles X_{AVK} have altitude resolution comparable to the GOME-2 profiles (or coarser).

Since the GOME-2 measurement alone does not fully constrain the retrieved ozone profile, GOME-2 profiles are a mix of measured information and a-priori "climatological" ozone profiles. At altitudes where the measurement provides tight constraints, the retrieved ozone comes to 80% or 90% of the measurement. At other altitudes (usually the troposphere and mesosphere), the GOME-2 profile comes to 80% or 90% of an a-priori profile. For the validation of the retrieval process, it makes sense to also consider reference profiles that have been smoothed by the averaging kernels, and have the same mix of measured and a-priori profile as the GOME-2 profiles. The resulting profiles are called $X_{AVK\ apriori}$ in the following.

In nearly all cases, the validation of GOME-2 profiles (Figure 2.2) gives almost the same results for the three version of smoothed reference profiles X_{ref}, X_{AVK}, and $X_{AVK\ apriori}$.

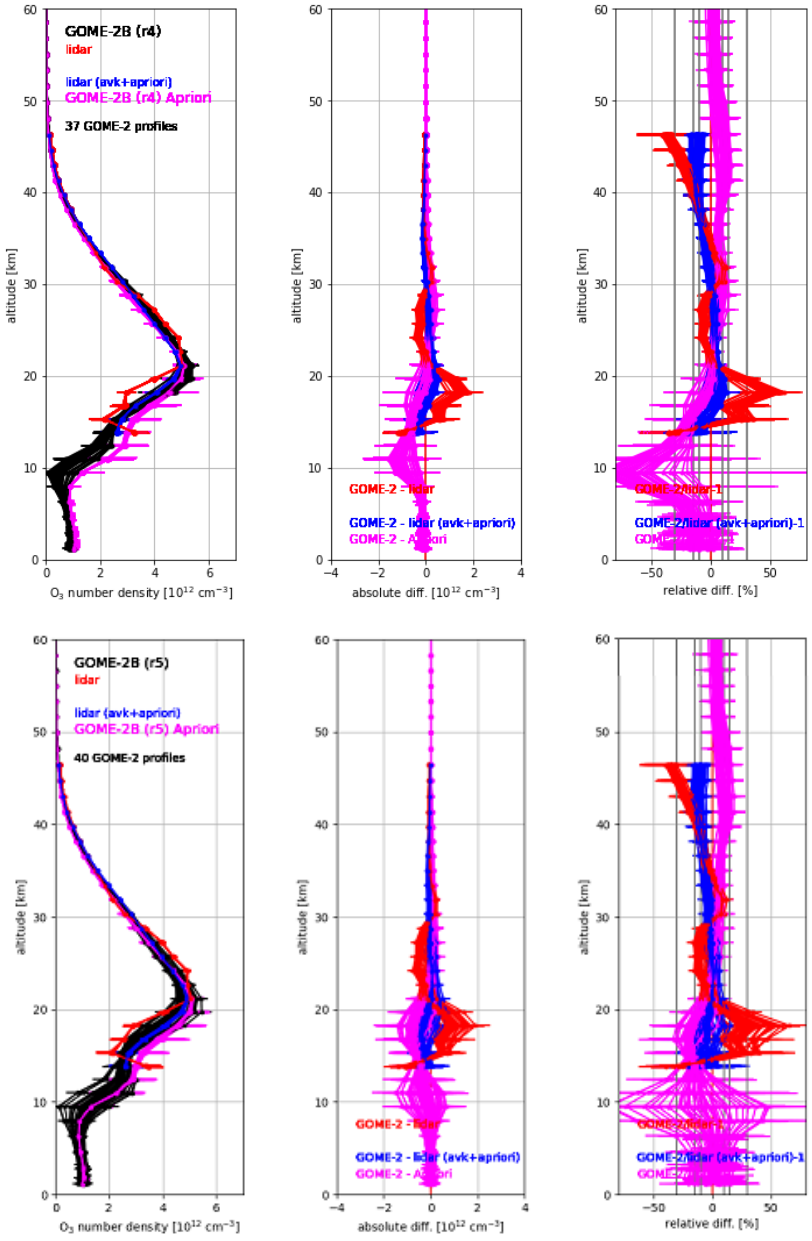

Figure 2.2: Example for the comparison of a lidar profile at Hohenpeissenberg (15.4.2013), Germany, (red X_{ref}, purple X_{avk}, blue $X_{avk,\ apriori}$) with the matching GOME-2 MetOp-B high-resolution profiles (black). Left panel: Profiles. Middle panel: Absolute differences. Right panel: Relative differences. Note that the GOME-2-layer altitudes and averaging kernels vary slightly from profile to profile. This results in small differences in the smoothed lidar profiles. Error bars (1σ) are from the reported measurement uncertainties for GOME-2 and lidar. The vertical lines at ±30%, ±15%, and ±10% in the right panel are the threshold, target, and optimum accuracies specified for the GOME-2 product. The upper panel shows the reprocessed data from 2019 and the lower panel the reprocessed data from 2023.

2.6 Results

This summary contains validation results for the reprocessed GOME-2A/B high resolution (HR) ozone profile products, retrieved by the Ozone Profile Retrieval Algorithm (OPERA) at KNMI. The validation period covers from January 2007 to August 2022 for MetOp A, from December 2012 to August 2022 for MetOp-B, and from January 2019 to August 2022 for MetOp C.

First we report the quality of GOME-2 ozone profile products in a very condensed way, the statistics for the different output levels of GOME-2 can be reduced to two layers: Lower Stratosphere (up to an altitude of 30 km) and Upper Stratosphere (above 30 km, up to 50 or 60 km). ***Table 2.2*** shows the definition of the height ranges for lower and upper stratosphere for different latitude belts used in this report.

Table 2.2: Definition of the ranges in km for lower and higher stratosphere for the different latitude belts.

	Lower Stratosphere	Upper Stratosphere
Polar Region	12 km – 30 km	30 km – 50 km
Mid-Latitudes	14 km – 30 km	30 km – 50 km
Tropical Region	18 km – 30 km	30 km – 50 km

The validation for the lower stratosphere is made using ground-based ozonesonde data as a reference. For the upper stratosphere, ground-based lidar, FTIR and microwave radiometer data are used as reference.

Relative differences (Eq. 1) are calculated against the ground-based reference data. Usually these are also convolved with the averaging kernels, including the a-priori contribution (Smoothed ground-based):

$$\frac{(\text{GOME-2} - \text{Smoothed ground-based})}{\text{Smoothed ground-based}} * 100 \qquad (1)$$

Tables 2.3 and 2.4 provide a comprehensive summary of the disparities between the reprocessed ozone profiles from GOME-2A and B in 2019 (considered the operational dataset) and the reprocessed ozone profiles from 2023 when compared to ground-based reference profiles. The evaluation spans from January 2007 to December 2018 for MetOp-A (Table 2.3) and from December 2012 to June 2018 for MetOp-B (Table 2.4). Statistical analyses are presented for both the lower and upper stratosphere, with earlier discussion on tropospheric ozone detailed in this report. Lower stratospheric statistics are sourced from KMI, while upper stratospheric statistics are derived from DWD.

In addition, Table 2.5 delves into the overall differences between GOME-2C operational and reprocessed ozone profiles for the timeframe spanning January 2019 to August 2022.

The optimum target of 10% accuracy, as outlined in the GOME-2 ozone profile ATBD, is achieved in both the lower and upper stratosphere across nearly all examined belts. When comparing the two reprocessed datasets for MetOp A and B, a marginal enhancement is noted in the polar region, while no improvement is observed in other belts. In the case of MetOp C, statistics indicate an improvement compared to the operational dataset. It is noteworthy to mention a consistent negative bias observed in all examined belts, with the most significant disparity noted in the tropics.

The time series in Figures 2.3 and 2.4 demonstrate that the reprocessed ozone data from GOME-2B achieves the same result as the reprocessed dataset from 2019 and now operational dataset. The same is true for GOME-2A (not shown) The timeseries shows the monthly difference between GOME-2B and the reference ground-based MWR and lidar station between 20 and 25 km and between 35 and 40 km altitude. The error of ECMWF hemisphere swap (2015 and 2016) was already corrected in the prvious reprocessed data set and also the more than 60% decade drift in the upper Stratosphere disappeard. However, in the late winter month at the Ny Alesund higher deviation between Gome-2B and the ground-based measurements are observed (Figure 2.4). The errors are slightly higher in the reprocessed data, a trend also evident in sections 2.3 and 2.4. Higher standard deviations are observed in the reprocessed dataset, particularly in polar regions.

Table 2.3: Absolute Differences (AD), Relative Differences (RD) and standard deviation (STDEV) of GOME-2A HR ozone profile products versus ground-based reference profiles for lower and upper stratosphere and different latitude belts. Results are for the time period January 2007 to December2018. The upper table is for HR data and the lower for the reprocessed data. Please note that the statistics include FTIR measurements compared to previous reports.

	GOME-2A HR operational					
	Lower Stratosphere			Upper Stratosphere		
	AD (DU)	RD (%)	STDEV (%)	AD (DU)	RD (%)	STDEV (%)
Northern Polar Region	-9.4	-3.4	14.3	-1.1	-2.8	14.9
Northern Mid-Latitudes	-2.2	-0.4	9.0	-1.6	-2.7	7.8
Tropical Region	1.8	2.1	9.2	-6.1	-8.1	4.5
Southern Mid-Latitudes	-4.8	3.3	14.8	-2.9	6.0	5.6
Southern Polar Region	-1.5	4.1	38.7	-	-	-

	GOME-2A HR reprocessed 2023					
	Lower Stratosphere			Upper Stratosphere		
	AD (DU)	RD (%)	STDEV (%)	AD (DU)	RD (%)	STDEV (%)
Northern Polar Region	-0.99	-4.34	14.05	-0.9	-0.3	16.1
Northern Mid-Latitudes	-0.18	-0.26	9.43	-2.1	-3.6	10.4
Tropical Region	0.26	2.19	8.78	-6.8	-8.9	4.3
Southern Mid-Latitudes	0.46	3.31	14.08	-3.3	-5.9	6.7
Southern Polar Region	-0.14	2.47	30.02	-	-	-

*The relative difference statistics are derived as a weighted average over the lower- and upper stratospheric ozone profile levels. The absolute differences however are integrated over respectively the lower- and upper stratospheric ozone profile levels.

Table 2.4: Absolute Differences (AD), Relative Differences (RD) and standard deviation (STDEV) of GOME-2B HR ozone profile products versus ground-based reference profiles for lower and upper

stratosphere and different latitude belts. Results are for the time period December 2012 to December 2018. The upper table is for HR data and the lower for the reprocessed data.

	GOME-2B HR operational					
	Lower Stratosphere			Upper Stratosphere		
	AD (DU)	RD (%)	STDEV (%)	AD (DU)	RD (%)	STDEV (%)
Northern Polar Region	0.1	1.3	27.2	-1.9	-2.6	10.9
Northern Mid-Latitudes	3.3	2.0	8.8	-1.0	-1.3	9.8
Tropical Region	7.0	5.5	8.3	-5.2	-9.4	5.8
Southern Mid-Latitudes	13.1	7.0	10.5	-2.7	-6.6	6.4
Southern Polar Region	6.8	8.8	59.4	-	-	-

	GOME-2B HR reprocessed 2023					
	Lower Stratosphere			Upper Stratosphere		
	AD (DU)	RD (%)	STDEV (%)	AD (DU)	RD (%)	STDEV (%)
Northern Polar Region	-0.13	0.22	17.94	-0.3	-0.1	15.4
Northern Mid-Latitudes	0.02	0.65	8.65	-1.9	-3.3	10.0
Tropical Region	0.65	4.33	8.33	-6.5	-10.5	4.8
Southern Mid-Latitudes	0.95	5.89	10.64	-3.6	-7.5	6.1
Southern Polar Region	-0.34	3.90	41.03	-	-	-

*The relative difference statistics are derived as a weighted average over the lower- and upper stratospheric ozone profile levels. The absolute differences however are integrated over respectively the lower- and upper stratospheric ozone profile levels.

Table 2.5: Absolute Differences (AD), Relative Differences (RD) and standard deviation (STDEV) of GOME-2C HR ozone profile products versus ground-based reference profiles for lower and upper stratosphere and different latitude belts. Results are for the time period January 2019 to August 2022. The upper table is for HR data and the lower for the reprocessed data.

	GOME-2C HR operational					
	Lower Stratosphere			Upper Stratosphere		
	AD (DU)	RD (%)	STDEV (%)	AD (DU)	RD (%)	STDEV (%)
Northern Polar Region	-0.68	-3.63	9.85	-4.6	-10.7	14.5
Northern Mid-Latitudes	-0.16	-0.12	8.17	-4.2	-7.3	10.3
Tropical Region	-0.09	0.28	5.55	-11.3	-14.6	5.8
Southern Mid-Latitudes	0.34	3.36	10.24	-8.1	-12.5	7.7
Southern Polar Region	0.09	14.47	57.47	-	-	-

	GOME-2C HR reprocessed 2023					
	Lower Stratosphere			Upper Stratosphere		
	AD (DU)	RD (%)	STDEV (%)	AD (DU)	RD (%)	STDEV (%)
Northern Polar Region	-0.33	-1.13	20.27	-2.9	-5.1	10.2
Northern Mid-Latitudes	-0.04	0.38	7.94	-3.4	-4.0	11.5
Tropical Region	0.05	1.04	5.61	-9.7	-11.6	5.3
Southern Mid-Latitudes	0.58	4.42	9.83	-5.3	-8.8	5.9
Southern Polar Region	-0.11	7.19	44.68	-	-	-

*The relative difference statistics are derived as a weighted average over the lower- and upper stratospheric ozone profile levels. The absolute differences however are integrated over respectively the lower- and upper stratospheric ozone profile levels.

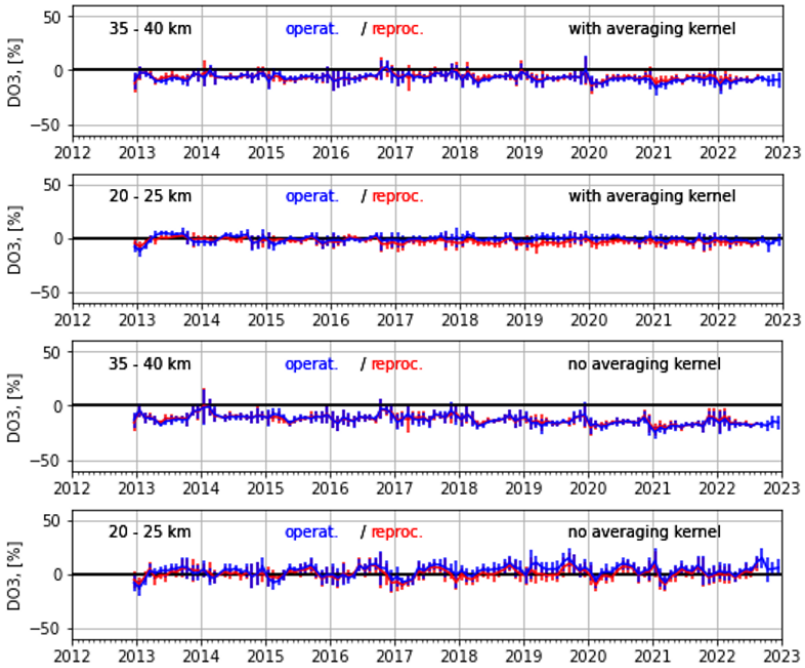

Figure 2.3: Time series of monthly mean difference with averaging (upper panel) and without averaging kernel (lower panel) between GOME-2 MetOp-B operational (blue) as well as reprocessed data (red) and NDACC lidar ground-based ozone measurements at Hohenpeissenberg.

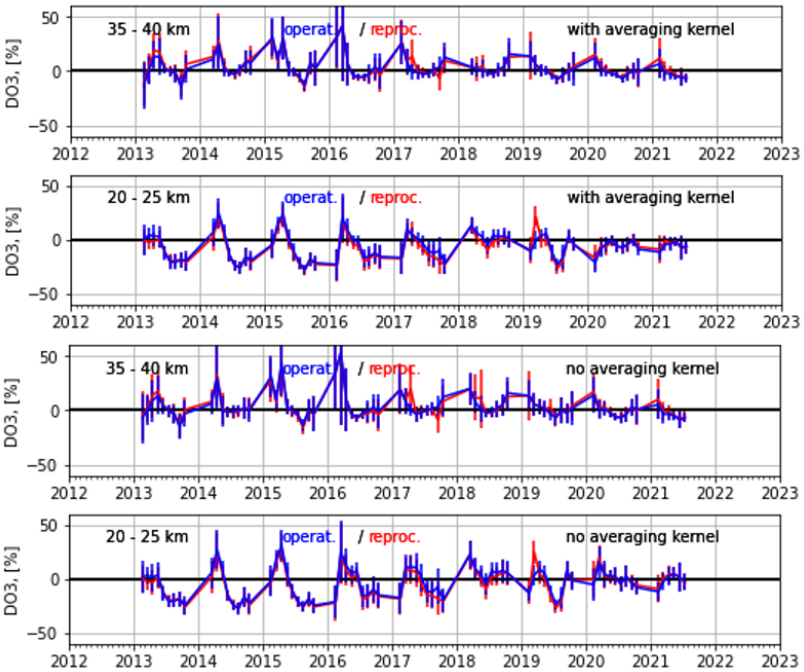

Figure 2.4: Time series of monthly mean difference with averaging (upper panel) and without averaging kernel (lower panel) between GOME-2 MetOp-B operational (blue) as well as reprocessed data (red) and NDACC ground-based MWR ozone measurements at Ny Alesund.

The time series depicted in Figures 2.5 illustrates the monthly discrepancies between GOME-2C and the reference ground-based lidar at Maunaloa within altitude ranges of 20-25 km and 35-40 km. The operational and reprocessed monthly differences are presented for comparison. Notably, there is a subtle enhancement observed in the upper atmosphere for the years 2019 and 2020. Additionally, there is a marginal improvement in errors within the reprocessed dataset. The same marginal improvements are also observed at other latitude bands (not shown).

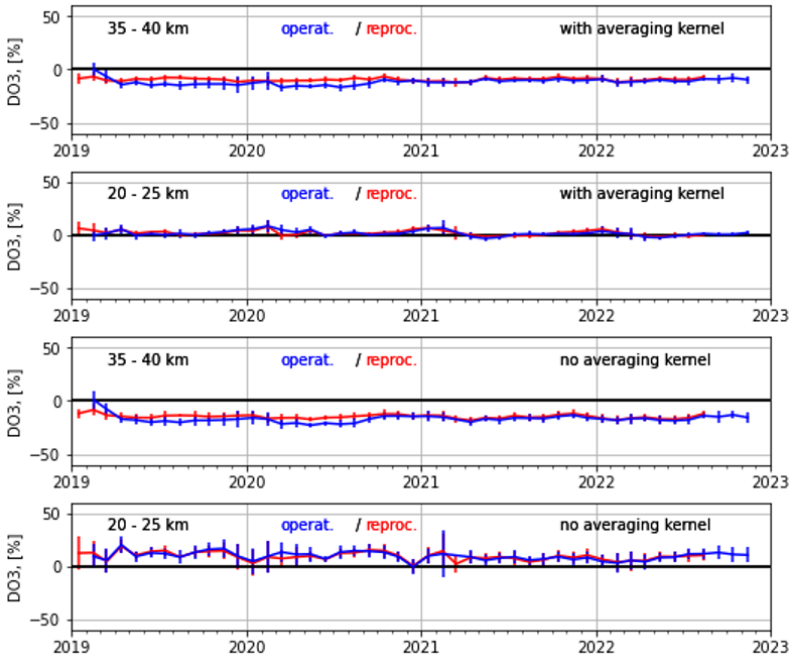

Figure 2.5: Time series of monthly mean difference with averaging (upper panel) and without averaging kernel (lower panel) between GOME-2 MetOp-C operational (blue) as well as reprocessed data (red) and NDACC ground-based MWR ozone measurements at Maunaloa.

Figure 2.6 shows an example of a comparison between a microwave profile measured at Ny Alesund on the 20.2.2016 with the matching GOME-2 MetOp-A high resolution profiles. In nearly all cases in late winter/early spring, the GOME-2 profiles (Figure 2.6) do not agree very well with the three version of smoothed reference profiles X_{ref}, X_{AVK}, and $X_{AVK\ apriori}$. There seams to be no improvement between the dataset from 2019 (operational data set, upper panel) and the new reprocessed data set from 2023 (lower panel).

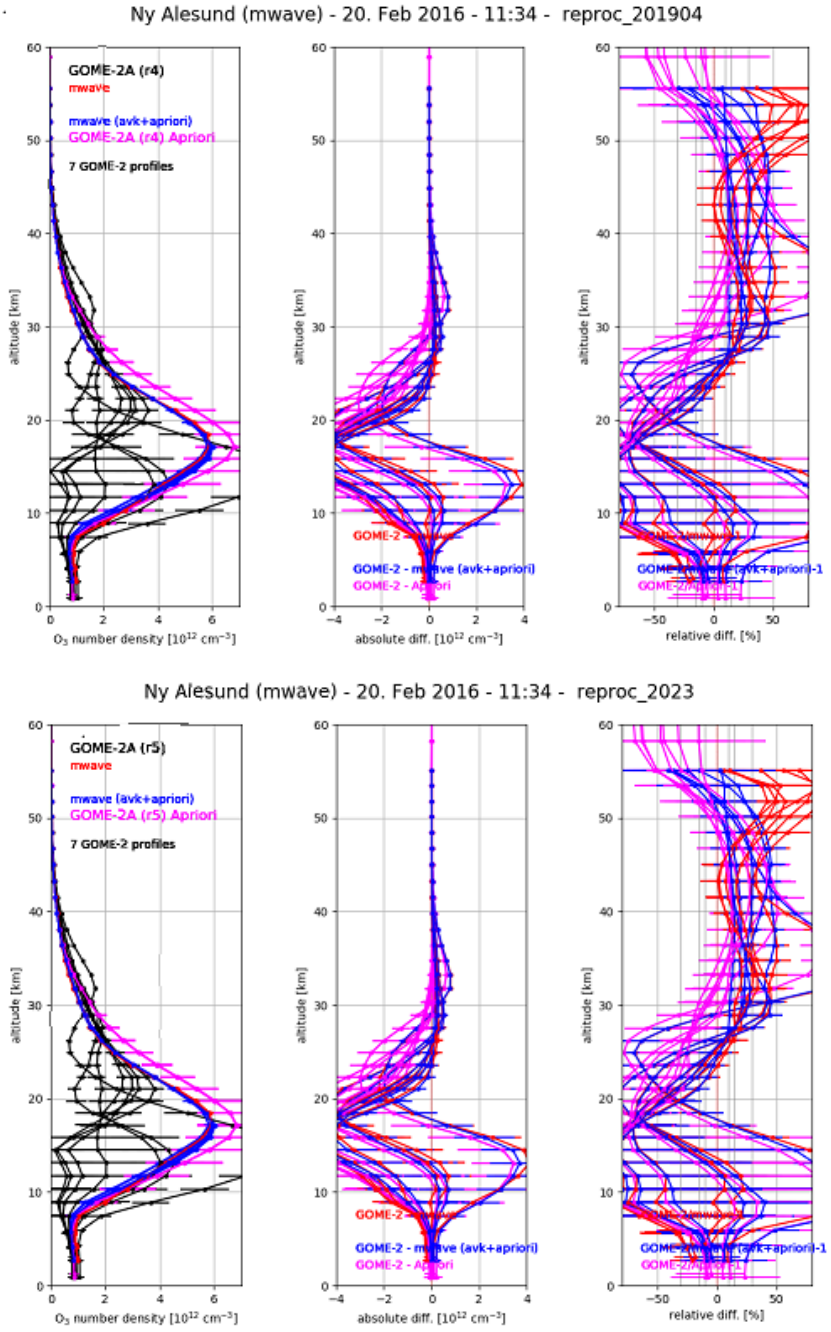

Figure 2.6: Example for the comparison of a microwave radiometer profile at Ny Alesund (20.2.2016), (red X_{ref}, purple X_{avk}, blue $X_{avk,\ apriori}$) with the matching GOME-2 MetOp-A high resolution profiles (black). Left panel: Profiles. Middle panel: Absolute differences. Right panel: Relative differences. Note that the GOME-2layer altitudes and averaging kernels vary slightly from profile to profile. This results in small differences in the smoothed microwave radiometer profiles. Error bars (1σ) are from the reported measurement uncertainties for GOME-2 and microwave radiometer. The vertical lines at ±30%, ±15%, and ±10% in the right panel are the threshold, target, and optimum accuracies specified for the GOME-2 product.

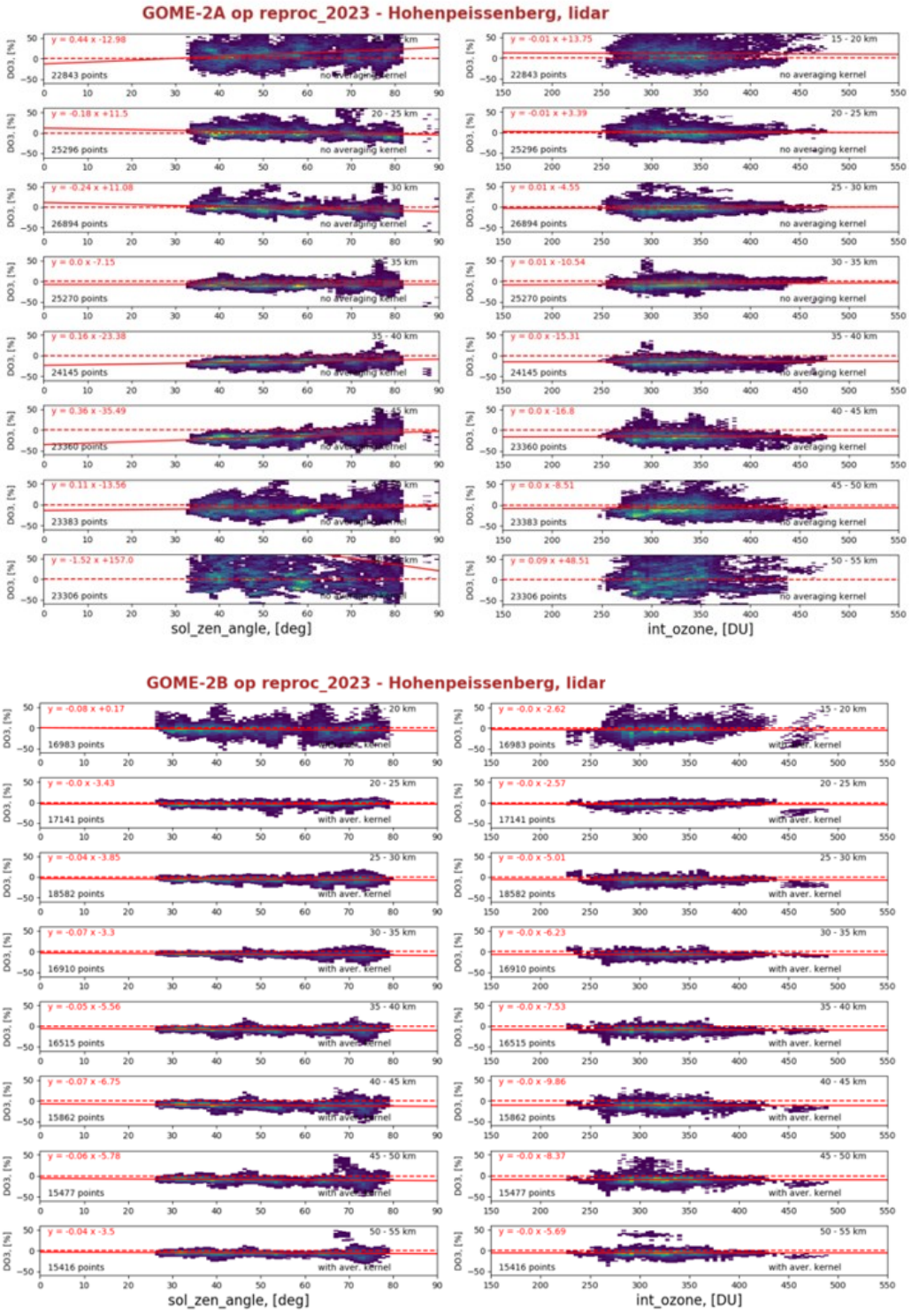

Figure 2.7: Scatter plot of ozone differences between GOME-2 MetOp-A (upper panel)/ Meteop-B (lower panel) – ground-based depending on solar zenith angle (left) and initial ozone column (right) at Hohenpeißenberg.

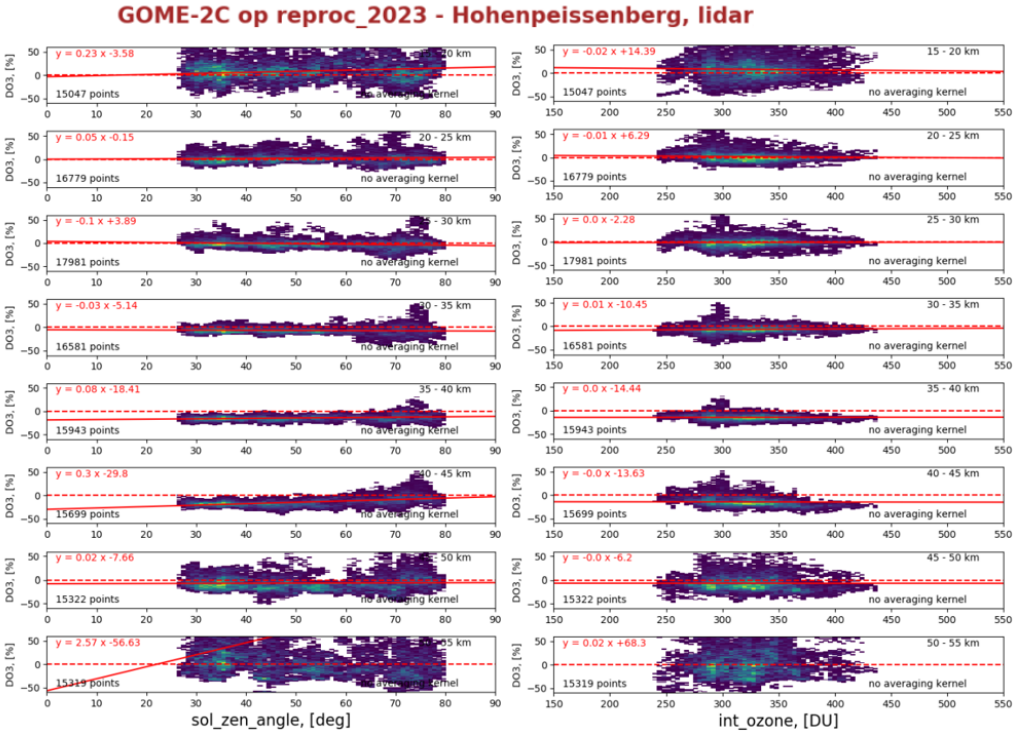

Figure 2.8: Scatter plot of ozone differences between GOME-2 MetOp-C – ground-based depending on solar zenith angle (left) and initial ozone column (right) at Hohenpeißenberg.

Figure 2.7 and 2.8 shows a comparison between GOME-2 ozone measurements and ground-based observations at Hohenpeißenberg, categorized by solar zenith angle and initial ozone column, across various altitude intervals. The statistics cover the period from January 2019 to August 2022. From Figure 2.7, it is noticeable that the reprocessed data from MetOp-A exhibit slight variations with solar zenith angle, whereas this phenomenon is not observed in the MetOp-B dataset. Additionally, for MetOp-C (Figure 2.8), a slight dependency with solar zenith angle is evident. The most pronounced dependency is observed for the lowest and highest altitude intervals. At polar latitudes (not shown), the highest dependency with solar zenith angle occurs at the lowest altitude intervals (15-20km, 20-25km, and 25 to 30km), while at mid-latitudes and in the tropics, the dependency is more prominent at higher altitudes. It's worth noting that for all satellites, no dependency with the initial ozone is observed. We also do not observe a dependency on the cloud fraction, scan angle, or temporal or spatial distance between satellite and ground-based measurement. At most altitudes there is also no indication for a significant variation with total ozone column. The only exception is the lower stratosphere at higher latitudes (not shown), where data from Ny-Alesund and Lauder indicate that below 25 km GOME-2 tends to underestimate ozone when the total ozone column is low, and tends to overestimate ozone when the total ozone column is high. An annual cycle variation has been observed with GOME-2A, B and C reprocessed ozone profile data at high latitudes.

2.7 Conclusions

Overall, these validation results affirm that GOME-2A, B, and C reprocessed ozone profiles exhibit good quality and comparability with the operational dataset. In the stratosphere, they meet the ±10% optimal accuracy goal across a broad range of conditions, and the ±15% target accuracy under almost all conditions. However, a noticeable increase in noise is observed in the reprocessed dataset, particularly in the polar regions of MetOp-A and B, evident through higher standard deviations. An avenue for further improvement lies in reducing the accuracy and uncertainty of the retrieval at high latitudes.

3 Integrated profiles validation using ground-based measurements

3.1 Dataset description

3.1.1 GOME-2/MetOpA, MetOpB and MetOpC integrated ozone profile data

The GOME-2/MetOpA, GOME-2/MetOpB and GOME-2/MetOpC data (hereafter GOME-2A, GOME-2B and GOME-2C) integrated ozone profiles were retrieved by the algorithm and using the methodology that is described in the "NRT, Offline and Data Record Vertical Ozone Profile and Tropospheric Ozone Column Producs" ATBD (Tuinder, 2022). The GOME-2 integrated ozone profile datasets used in this validation report cover the following time periods:

- GOME-2A: 4 January 2007 – 15 November 2021
- GOME-2B: 29 October 2012 – 31 August 2022
- GOME-2B: 3 January 2019 – 31 August 2022

The datasets were provided by the KNMI algorithm team in the form of overpass files for a specified number of ground-based stations.

To further establish the validation results of the GOME-2A, -2B and -2C integrated ozone profiles, they are also compared to the respective operational total ozone column (TOC) products retrieved by the GDP v.4.8 (GDP v4.9 for GOME-2C) algorithm.

3.1.2 Ground-based data

The ground-based measurements database used for this validation report consists of archived Brewer and Dobson total ozone data that are downloaded from the World Ozone and Ultraviolet Radiation Data Centre (http://www.woudc.org). WOUDC is one of the World Data Centers which are part of the Global Atmosphere Watch (GAW) program of the World Meteorological Organization (WMO). These data are quality controlled, first by each station and secondly by WOUDC.

To ensure the high quality of the reference ground-based data used for this validation report, updated information was extracted from recent inter-comparisons and calibration records. This continuously updated selection of ground-based measurements has already been used numerous times in the validation and analysis of global total ozone records such as the inter-comparison between the OMI/Aura TOMS and OMI/Aura DOAS algorithms (Balis et al., 2007a), the validation of ten years of GOME/ERS-2 ozone record (Balis et al., 2007b), the validation of the updated version of the OMI/Aura TOMS algorithm (Antón et al., 2009), the GOME-2/MetOp-A validation (Loyola et al., 2011; Koukouli et al., 2012), the GOME-2/MetOp-B validation (Hao et al., 2014), the evaluation of the European Space Agency's Ozone Climate Change Initiative project (O3-CCI) TOCs (Koukouli et al., 2015, Garane et al., 2018) and the validation of the TROPOMI/S5P total ozone products (Garane et al., 2019). In all the aforementioned publications, LAP/AUTH assumes the leading role in the validation efforts.

In this report, archived data for the period **January 2007 to August 2022** are used for the comparisons, depending on the availability of data for each individual station. The Brewer and Dobson WOUDC stations considered for the comparisons are listed in Tables A.1 and A.2 (Appendix 1) and their geographical distribution is depicted in Figure 3.1. In Figure 3.2, the distribution of the co-located ground-based measurements in space in time are shown for the three sensors (GOME-2A in the first row, GOME-2B in the second row and GOME-2C in the third row).

In the comparison plots and statistics presented in this report, only the direct sun observations provided by the Brewers and Dobsons are utilized for the computation of the percentage differences between satellite and co-located ground-based measurements, since they are considered of higher accuracy than all the other types of ground-based observations. Finally, only northern hemisphere Brewer ground-based stations are considered, because the number of stations in the southern hemisphere is very limited and they are mainly located in Antarctica.

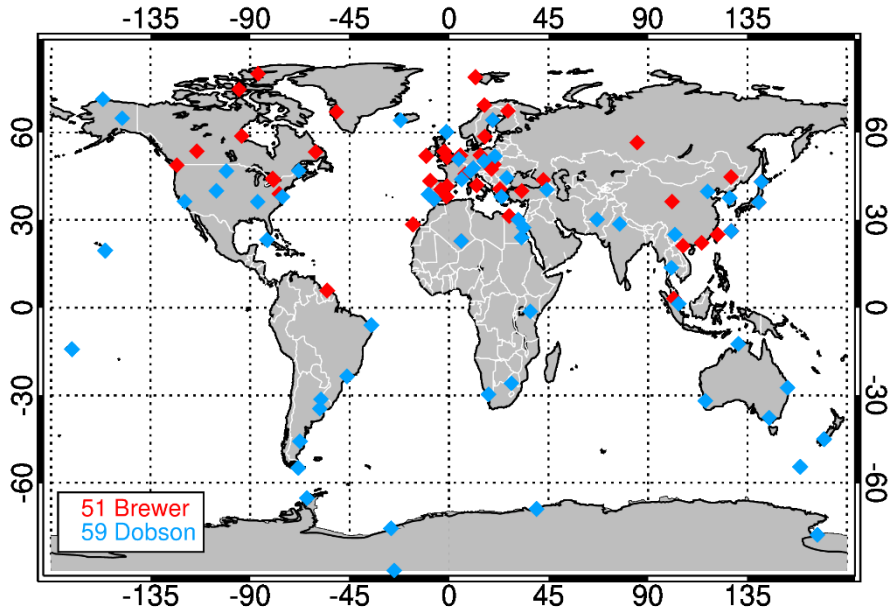

Figure 3.1: Spatial distribution of the Brewer and Dobson ground-based stations used for the comparisons.

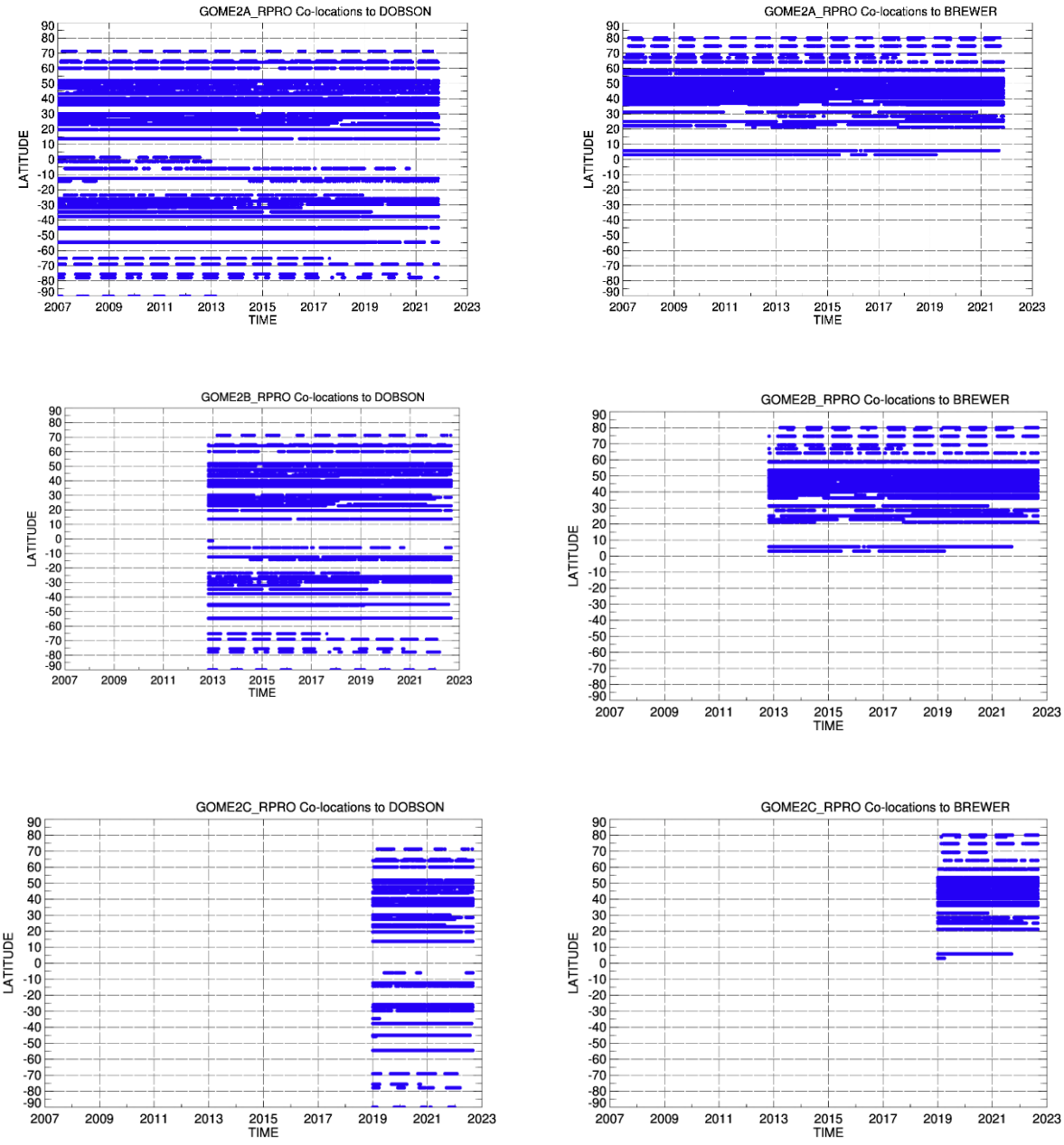

Figure 3.2 : Spatial and temporal representation of the co-location data used for the validation with ground-based measurements (left panels: Dobson, right panels: Brewer) for the time period of the GOME-2A (first row), GOME-2B (second row) and GOME-2C (third row) operation until August 2022.

3.2 Validation of the reprocessed GOME-2 integrated ozone profiles

In this section, the archived and quality-controlled Dobson and Brewer daily total ozone measurements downloaded from WOUDC for the period January 2007 to August 2022, are used as ground-truth for the validation of GOME-2A, GOME-2B and GOME-2C reprocessed integrated ozone profiles. The datasets of the three satellite sensors are temporally and spatially co-located to ground-based measurements using the following **co-location criteria**:

- the satellite and daily ground-based total ozone measurements must correspond to the same day, and
- the maximum search radius between the ground-based stations and the centre coordinates of the satellite pixel is set to 150 km. The spatially closest satellite observation is paired with the ground-based station's daily-mean measurement.

This is a rather different approach compared to the validation methodology used in the previous sections, where each ground-based profile is compared with more than one co-located satellite profiles, but it is an established methodology followed in many total ozone validation reports in the past (either for integrated ozone profiles or for the operational products), as well as in numerous published papers for total ozone column validation (for example, Koukouli et al., 2015; Garane et. al. 2018; Garane et. al, 2019; Garane et al., 2020). Namely, in the work of Garane et al, 2019, different sampling strategies have been compared for the validation of TROPOMI/S5P total ozone columns, where individual measurements from the EUBREWNET Brewers were used along with the WOUDC dataset of daily mean ground-based measurements, with no significant differences in the validation results.

The pairs of co-located satellite and daily-mean ground-based measurements are used to calculate their percentage difference by the simple formula:

$$Diff\ (\%) = \frac{(satellite - ground)}{ground}\%$$

The datasets of percentage differences are then filtered:

- for solar zenith angle (SZA), which is limited up to 83°, because the mean percentage differences of the co-locations with SZA above 83° were higher than -10 %. The number of co-locations affected by this filtering criterion is ~ 1.5 % of the total.
- for latitude, which is limited up to 85° S because the mean percentage differences of the co-locations with latitude above 85° S were higher than +20 %. The number of co-locations affected by this filtering criterion is below 0.7% of the total.

The monthly means that are shown in the respective time-series plots are calculated by averaging the total number of available co-locations per month. Furthermore, the error bars in the following plots (where they are shown) stand for the 1σ standard deviation of the means.

Figure 3.3 shows the overall statistical analysis of the GOME-2A (panels a and b), GOME-2B (panels c and d) and GOME-2C (panels e and f) reprocessed integrated ozone profiles' co-locations to Brewer ground-based total ozone measurements. In the left column of figures, the distributions of the percentage differences of the co-locations are shown to be normal around the centre value, which is **0.8% for GOME-2A (panel a), 1.4% for GOME-2B (panel c) and ~1% for the GOME-2C (panel e) comparisons**.

The scatter plots, shown to the right, reflect the very good overall agreement of all sensors' integrated ozone profiles to the ground-based TOC measurements from Brewer instruments (**Pearson correlation coefficients > 0.97**). The respective correlation coefficients for the Dobson comparisons (not shown here for reasons of brevity) are greater than 0.96, resulting from nearly 89.200 (for GOME-2A), 61.500 (for GOME-2B) and 18.500 (for GOME-2C) co-locations, respectively.

A. Temporal evolution of the GOME-2A, GOME-2B and GOME-2C comparisons to ground-based measurements

Figure 3.4 shows the hemispherical full time series of the monthly mean percentage differences of GOME-2A (in blue), GOME-2B (in green) and GOME-2C (in red) integrated ozone profiles with respect to the co-located (in space and in time) ground-based measurements. The comparisons to Dobson measurements are shown in panels a (northern hemisphere) and c (southern hemisphere), while in panel b the Brewer comparisons are displayed (northern hemisphere only).

The first noticeable feature of the GOME-2A time-series is the abrupt change of level in the comparisons during the second half of 2013, which is present in both Brewer and Dobson co-locations and in both hemispheres. On the 15th of July 2013, the GOME-2A swath width changed from 1920 to 960 km. This means that the instrument now has more pixels in a more nadir direction than before, which can lead to a change in the averaged ozone profile in case there is a cross track bias. Additionally, in mid-2013 there is a discontinuity in the degradation correction because it is cross-track-pixel / scan angle dependent. As a result, in Table 3.1, the GOME-2A time-series is studied separately, before and after mid-2013, in terms of mean bias of the differences to ground-based measurements.

Moreover, due to the GOME-2A loss of solar visibility and the adaptation of an empirical model during the winter months (November - March) of 2018-2019, 2019-2020, and since August 2020 until the end of its mission, the GOME-2A time series for these time periods, as well as the respective statistics, are quite noisy (higher overall mean standard deviation by ~ 0.5 % compared to GOME-2B and GOME-2C). This is more pronounced in panel b where Brewer total ozone measurements are used as reference due to their lower seasonal dependency.

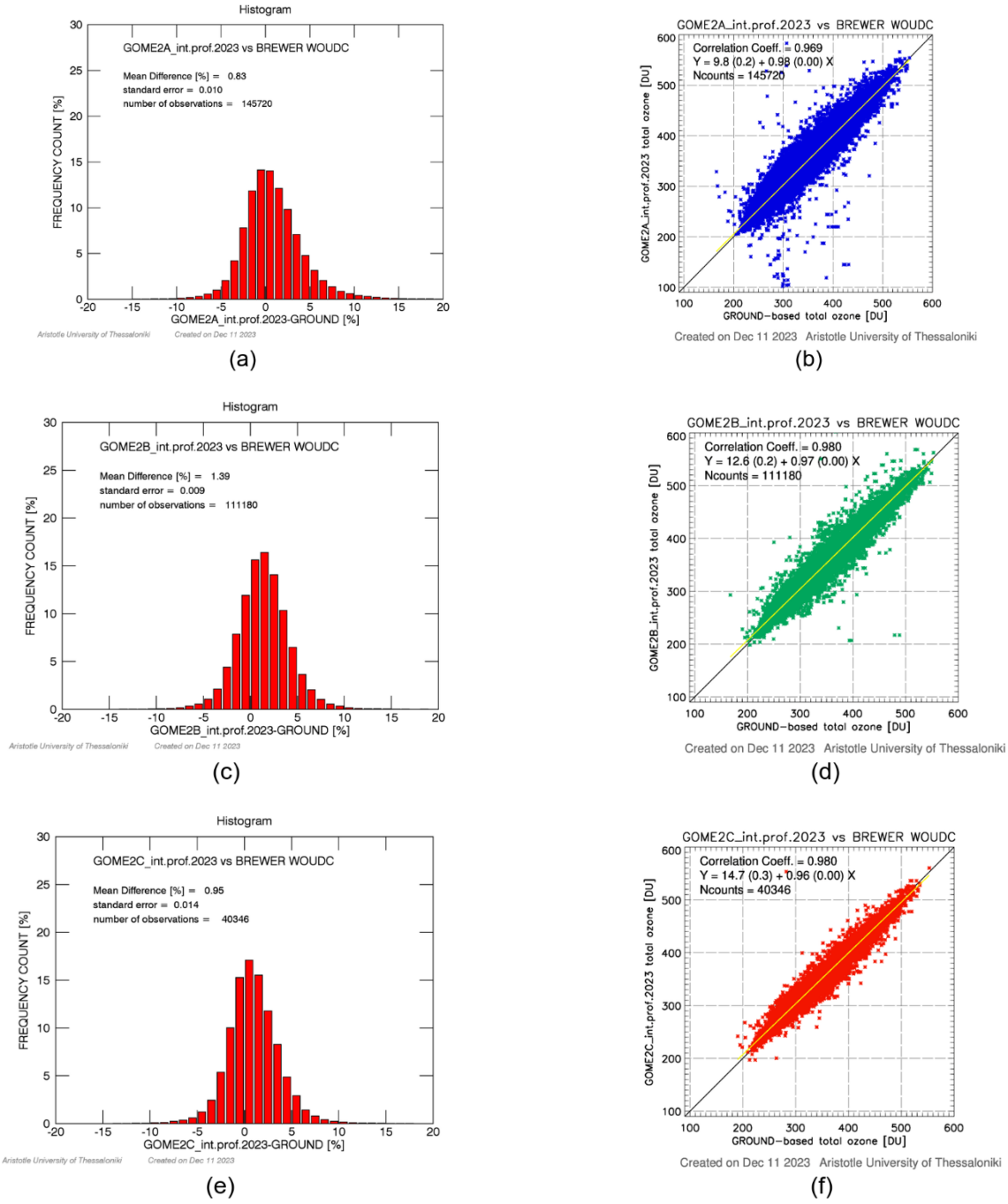

Figure 3.3 : Left panels: Histograms showing the distributions of the percentage differences of the GOME-2A (panel a), GOME-2B (panel c) and GOME-2C (panel e) co-locations to Brewer ground-based total ozone measurements. Right panels: Scatter plots of the co-located GOME-2A (panel b), GOME-2B (panel d) and GOME-2C (panel f) integrated ozone profile to ground-based TOC measurements from Brewer instruments.

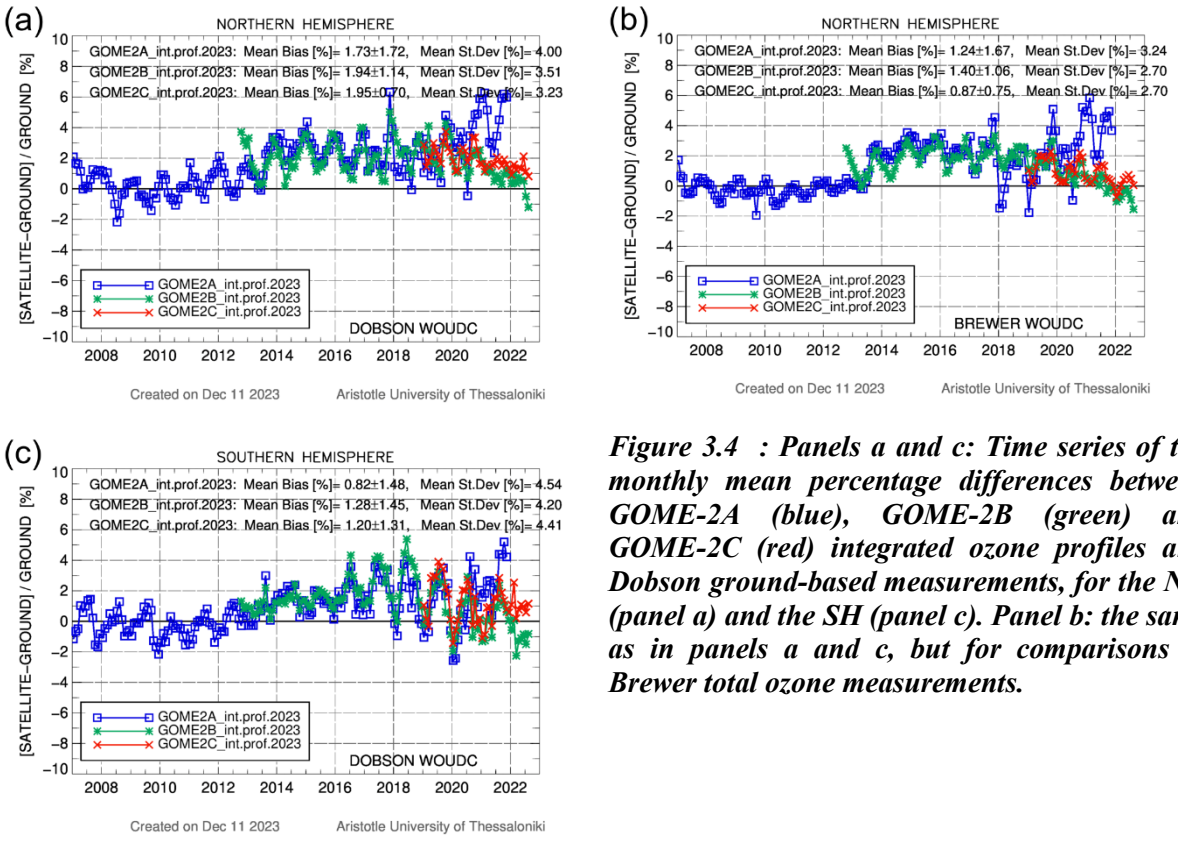

Figure 3.4 : Panels a and c: Time series of the monthly mean percentage differences between GOME-2A (blue), GOME-2B (green) and GOME-2C (red) integrated ozone profiles and Dobson ground-based measurements, for the NH (panel a) and the SH (panel c). Panel b: the same as in panels a and c, but for comparisons to Brewer total ozone measurements.

Another interesting point seen in Figure 3.4 (panel b) is the enhanced seasonality of the GOME-2B differences to Brewer[1] ground-based measurements compared to the seasonality of GOME-2A comparisons. The two instruments have possible differences in their calibration and use different wavelength ranges for the retrieval of the ozone profiles, which can lead to different total ozone columns, therefore this feature is expected.

The **decreasing bias of GOME-2B and GOME-2C** since 2020, which is seen in both hemispheres and with respect to both types of ground-based instruments, is another prominent feature. To further investigate the quality of the reprocessed integrated ozone profiles and to verify this decrease in bias since 2020, the operational GOME-2A, GOME-2B and GOME-2C total ozone column products retrieved with the algorithm GDP v.4.8 (GDP v4.9 for GOME-2C), are indirectly compared to the respective integrated ozone profiles via their co-locations to the same ground-based measurements. In Figure 3.5 the three sensors' time series with respect to Brewer ground-based measurements are seen. In all panels, the blue time series

[1] The seasonality feature of the percentage differences to ground-based measurements is principally studied using Brewers, because the Dobson measurements are known to be highly affected by the effective temperature (see Koukouli et al., 2016).

represents the respective integrated ozone profiles, and the red line shows the operational (GDP) total ozone product. The conclusions derived from these figures are:

- **GOME-2A** (panel a):
    1. First of all, comparing the two products, it is seen that the 2013 swath width change does not affect them in the same way. The operational product has a similar bias (before and after) but a narrower seasonal dependency after mid-2013. The reprocessed integrated ozone profiles retain the same seasonality but increase in bias by ~ 2.5%.
    2. Since mid-2016, the operational product starts to drift to continuously lower biases until the end of the mission in November 2021. The product under validation does not follow this decrease.

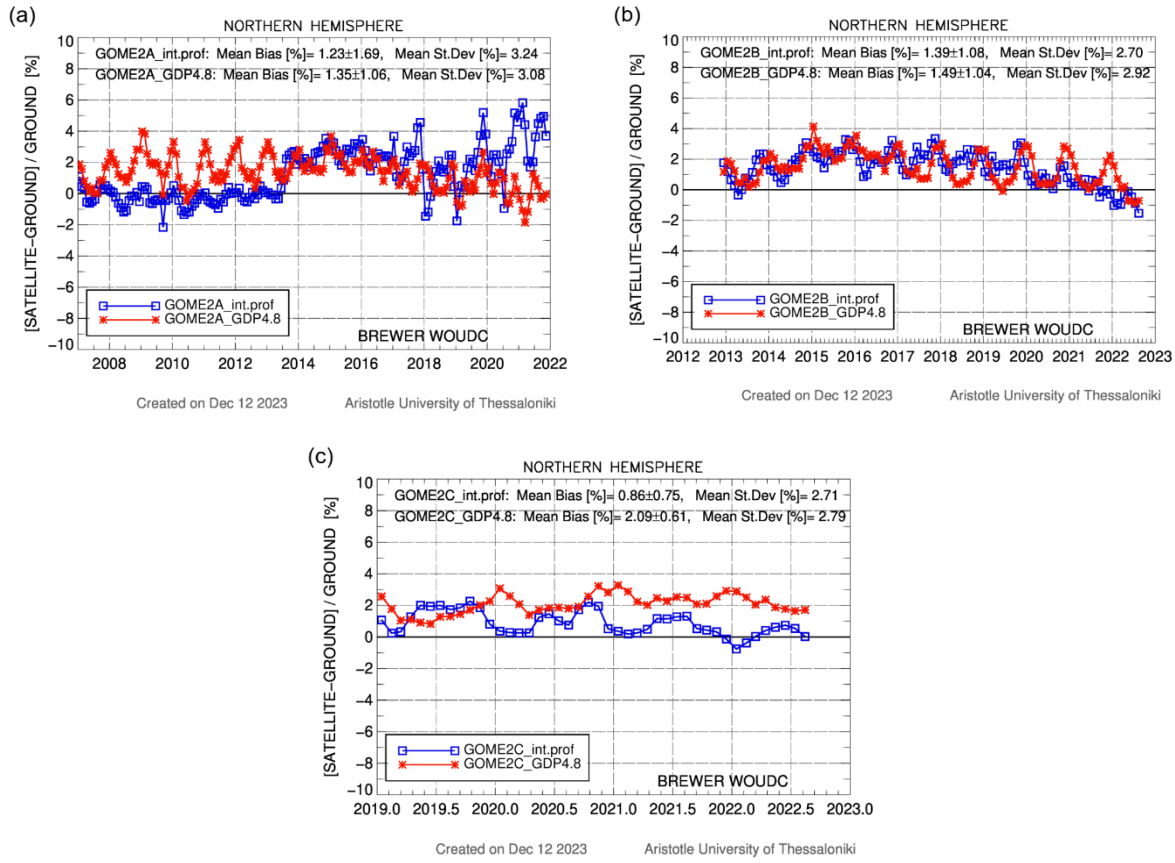

Figure 3.5: The monthly mean time series of the three sensors' time series with respect to Brewer ground-based measurements: GOME-2A in panel a, GOME-2B in panel b and GOME-2C in panel c. In all panels, the blue time series represents the respective integrated ozone profiles, and the red line shows the operational (GDP4.8 or 4.9 for GOME-2C) total ozone product.

3. The loss of solar visibility during the aforementioned time-periods, affects the integrated ozone profiles in a more intense way, strongly increasing the noise in the comparisons to ground-based measurements.

- **GOME-2B** (panel b): the agreement of the two products is excellent (within 0.5%) until the spring of 2017. Since summer 2017 the operational total ozone has lower mean relative biases during summer months, thus a higher seasonal dependency than the reprocessed integrated ozone profile. Besides that, the decreasing drift due to the instrument degradation since early 2020 is a common feature that is currently under investigation by the GDP algorithm team.
- **GOME-2C** (panel c): during 2019, the agreement between the operational and the product under validation is within ±1%. Since 2020, this difference increases continuously due to the decreasing percentage differences of the integrated total ozone with respect to the reference measurements. GOME-2C GDP4.9 total ozone has a mean bias of +2% which is temporally stable, even though it has a seasonality of 1.5% peak-to-peak. The reverse seasonal dependency of the two products is also interesting: the operational total ozone is biased higher during winter months (November – February), while the integrated total ozone has almost no bias during winter months, but during May-September the bias becomes also positive and up to 2%.

Nevertheless, the differences in the overall mean relative biases (statistics shown at the top of the figures) are very limited, up to 0.5% for GOME-2A and -2B, up to 1.2% for GOME-2C, in both hemispheres with respect to both types of ground-based instruments, which is very positive considering the differences in the retrieval methodologies.

The mean relative biases ± 1σ (in %) and mean standard deviations for GOME-2A (before and after mid-2013), GOME-2B and GOME-2C integrated ozone profiles with respect to ground-based measurements from Brewer and Dobson instruments, are summarized in **Error! Not a valid bookmark self-reference.**. It should be noted that the standard deviation of the comparisons represents the combination of the sensors' and the ground-based measurements' variability.

- Since the start of its operation until mid-2013, GOME-2A has a mean relative bias of ~ ± 0.3 %. For the second part of its time series, the mean relative bias increases to ~ +2.5 % and the mean standard deviation also increases by about 0.5% with respect to the previous time period, to ~3.5%. When excluding the winter months of the switch to the solar model, the mean relative bias after mid-2013 becomes slightly lower, + 2.2 %, but the mean standard deviation, thus the variability of the comparisons, reduces by 0.5% and becomes almost equal to the respective standard deviation of the 2007-2013 time period.
- GOME-2B and GOME-2C are very similar in terms of mean relative bias, which is 1.0 – 2.0 % for the NH, depending on the reference instrument, and ~1.2% for the SH. The mean standard deviation is also almost equal for the two instruments, 3-3.5% for the NH and ~4.3% for the SH, where the number of Dobson stations is lower.

Table 3.1 : The statistical analysis (mean relative bias in % ± mean standard deviation in %) of the comparisons of GOME-2A (before and after 2013), GOME-2B and GOME-2C integrated ozone profiles to Dobson and Brewer ground-based total ozone measurements, for their time period of operation until August 2022 (November 2021 for GOME-2A).

	Sensor:		**GOME-2A**		**GOME-2B**	**GOME-2C**
Reference	**Time period:**		**2007-2013**	**2013-2021**	**2012 – 2022**	**2019-2022**
DOBSON	NH	Bias ± 1σ %	+0.3 ± 0.9	+2.8 ± 1.4	+1.9 ± 1.1	+2.0 ± 0.7
		St. Dev. %	3.8	4.2	3.5	3.2
	SH	Bias ± 1σ %	-0.2 ± 0.8	+1.6 ± 1.4	+1.3 ± 1.5	+1.2 ± 1.3
		St. Dev. %	4.4	4.7	4.2	4.4
BREWER	NH	Bias ± 1σ %	-0.2 ± 0.6	+2.4 ± 1.4	+1.4 ± 1.1	+0.9 ± 0.8
		St. Dev. %	2.9	3.5	2.7	2.7

B. Latitudinal dependency of the comparisons

For the purposes of this validation report, in Sections B and C only the temporally common GOME-2A, GOME-2B co-locations to ground-based measurements are used to achieve the comparability between the datasets. This means that (a) GOME-2A is temporally restricted to October 2012 – November 2021, to match the GOME-2B record, which is also restricted to up until November 2021 and (b) it is verified that only days with available co-locations for both sensors are kept within the dataset. The reason for this restriction is to have two utterly comparable datasets, in terms of the influence variables that are studied onwards, such as latitude, solar zenith angle, clouds, etc. GOME-2C covers only 3.5 years, hence the dataset is used in its entirety.

In Figure 3.6 the percentage differences between the reprocessed ozone integrated profiles retrieved by the three sensors and the TOC measurements from Dobson (panel a) and Brewer (panel b) ground-based instruments, are averaged in 10° latitude bins and plotted versus latitude. As it follows from the figures, both sensors have higher differences to ground-based measurements in the tropics and mid-latitudes, with mean relative biases of ~ 2.5% within ±50°. Closer to the northern high latitudes the biases decrease to ~1%. In the southern hemisphere, below 70° S, the bias becomes highly negative for all three sensors up to -2.5% for GOME-2A and GOME-2B, and up to -4.5% for GOME-2C. Higher negative biases in this area of the southern hemisphere with respect to Dobson measurements, is a frequently seen feature, therefore it raises no particular concern.

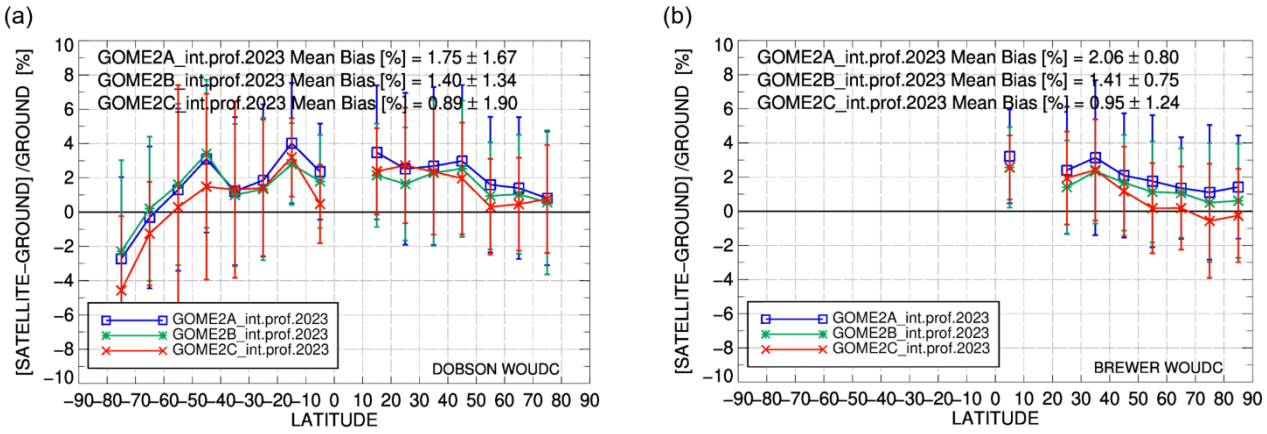

Figure 3.6: The latitudinal dependency of the percentage differences between the ozone integrated profile retrieved by the three sensors (GOME-2A, GOME-2B and GOME-2C) and the TOC measurements performed by Dobson (panel a) and Brewer (panel b) ground-based instruments.

C. Dependence on SZA and other influence quantities

The dependence of the percentage differences on solar zenith angle (SZA) is shown in Figure 3.7 for the Brewer comparisons (northern hemisphere stations only) that have a narrower annual cycle:

- GOME-2A is almost independent of SZA and has a very stable mean relative bias of ~ +1.9 %.
- GOME-2B is slightly dependent on SZAs < 75° with a mean relative bias of +1.6%, but the comparisons start to decrease and become negative above 75° (mean rel. bias: -0.3 %).
- GOME-2C has a very similar pattern to GOME-2B but with lower biases up to ~ +1.5 % above 50°. Overall, GOME-2C has a mean relative bias of +1.2 % for SZAs< 80°, that becomes -1.4 % above 80°, and has a stronger dependency on SZA compared to the other two sensors.

It is worth mentioning that according to the Product Requirements Document (Hovilla et. all, 2019), the **accuracy requirements** for the GOME-2 MetOp-A, MetOp-B and MetOp-C Total Ozone products are 4% for SZAs < 80° and 6% for SZAs > 80°. As seen in Figure 3.7, the GOME-2A, -2B and -2C accuracy is well these target values, which proves that the reprocessed integrated ozone profiles product is of similar quality to the operational GOME-2 total ozone column products.

For the purposes of this report, the effect of many influence quantities, such as cloud parameters, surface albedo etc., on the validation results was studied and no unexpected dependences were found.

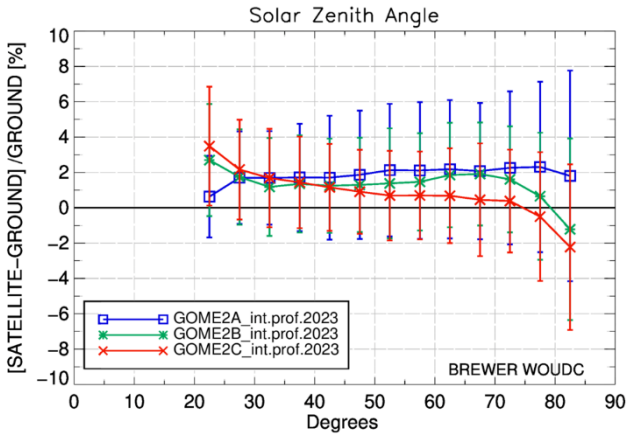

Figure 3.7 : The dependence of the percentage differences on solar zenith angle. Left panel: the Dobson comparisons, right panel: the Brewer comparisons.

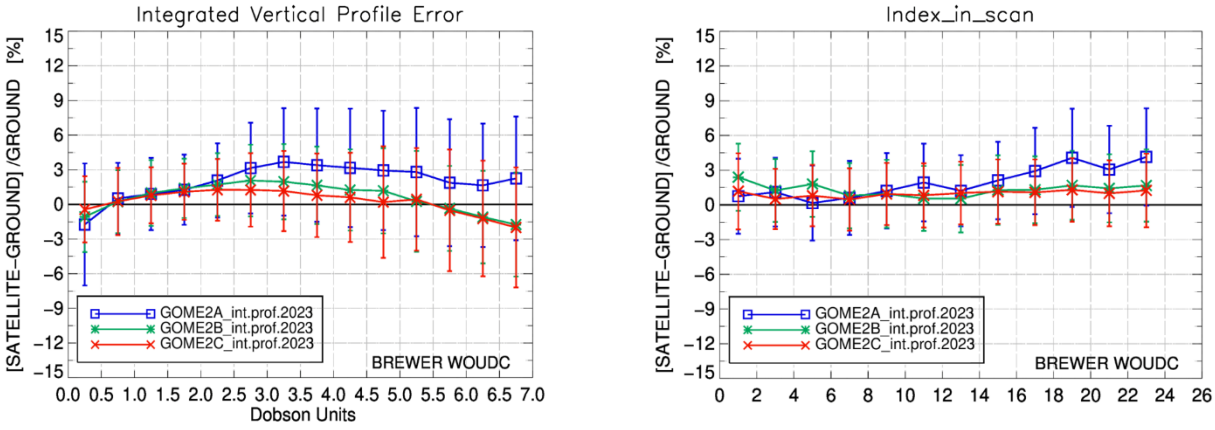

Figure 3.8: The dependence of the percentage differences on the integrated vertical profile error (left panel) and the Index In Scan of the measurements (right panel) with respect to Brewer TOC measurements.

An interesting feature that was seen during this validation exercise, is the dependence of the percentage differences on the integrated vertical profile error, seen in Figure 3.8, left panel. The majority of the co-locations correspond to measurements with error values spanning 0.5 - 3.5 DU. It is noticed that GOME-2B and GOME-2C depend on the products' error similarly: the biases increase up to +1.5 % for error values up to 2 DU and remain almost stable until the error becomes greater than 5 DU. Then the biases turn negative, up to -1.5 %. GOME-2A has a different pattern: there is also an increasing mean bias for errors up to 2.5 DU, but the bias remains stable (~ +3 %) after that value, regardless of the error values.

Moreover, in the right panel of Figure 3.8, the dependence of the percentage differences on the index in scan of the measurements, is shown. GOME-2B and GOME-2C, as before, have a

similar behaviour with no dependency on the index in scan, being almost stable at the +1.3 % level. On the contrary, GOME-2A for index values above 14 increases reaching +3 %.

The dependencies of the integrated ozone profiles on the integrated vertical profile error and the index in scan seen in these figures is a mixture of numerous ozone profile parameters and is currently under investigation by the algorithm team.

3.3 Conclusions from the reprocessed integrated ozone profile validation

The GOME-2A, GOME-2B and GOME-2C reprocessed integrated ozone vertical profiles were validated using ground-based daily total ozone measurements from Dobson and Brewer instruments, downloaded from WOUDC.

The validation results can be summarized to the following points:

- The comparisons of the two sensors had to be filtered for latitude. Their co-locations with Dobson ground-based measurements with latitude greater than 85° S had a mean percentage difference of ~ +20 %. This indicates that there is a serious difficulty with the products' retrieval algorithm in the Southern high latitudes that should be studied and resolved. Likewise, the comparisons with SZA > 83° had to be excluded, because their ~ -10 % mean bias introduced a lot of noise in the measurements and their statistics.
- The GOME-2A reprocessed integrated ozone profile time-series had to be studied separately before and after mid-2013, when the change in its swath and a discontinuity in the degradation correction occurred and affected the retrieval algorithm.
- The **statistical analysis** (mean bias in % ± mean standard deviation in %) of the GOME-2A and GOME-2B comparisons to co-located (in space and in time) Dobson and Brewer ground-based measurements is shown in Table 3.1, where it can be seen that the GOME-2A integrated ozone profile product agrees very well (difference up to ± 0.3%) with the ground-based data before mid-2013. The bias increases to +2 % after that point. Overall, GOME-2B has a mean bias of ~+1.5 to +2% and reports slightly lower integrated ozone vertical profile values (by up to 1%) compared to GOME-2A (after mid-2013). GOME-2C has very similar mean biases and variability to GOME-2B.
- The reprocessed GOME-2 integrated ozone profile products where indirectly compared to the respective operational total ozone products processed with the GDP4.8 (or GDP4.9 for GOME-2C) algorithm to further assess their consistency.
    - GOME-2A integrated ozone profiles were found to underestimate total ozone with respect to GDP4.8 by 2.5 % before mid-2013 in both hemispheres. Also, the loss of solar visibility of GOME-2A since 2018 is affecting the two products differently, increasing the variability of the integrated total ozone especially after mid-2019.

- GOME-2B agrees well with the GDP4.8 TOC product, within 0.5%. During 2017 - 2019 their timeseries start to deviate up to 1% during summer months. Since 2020 these deviations are shifted towards winter months and increased up to 2%.
- As for GOME-2C, the decreasing tendency of the integrated total ozone with respect to the reference measurements is not a feature seen in the respective GDP4.9 total ozone comparisons, which are temporally stable.

- The latitudinal analysis of the comparisons showed that all sensors have increased bias with respect to ground-based measurements in the tropics and mid-latitudes, up to 2.5 – 3%.
- The dependency of the comparisons on SZA showed very similar features for GOME-2B and GOME-2C, but almost no dependency for GOME-2A.

In conclusion, the validation of the GOME-2A, GOME-2B and GOME-2C reprocessed integrated ozone profiles with respect to Dobson and Brewer ground-based total ozone measurements, shows that the quality meets the requirements. The step function in the GOME-2A time-series during mid-2013 does not make it suitable for long term studies, but the overall good agreement of both sensors to ground-based measurements, to the respective operational products, and the luck of severe dependencies on various influence quantities, is an additional proof of the good quality of the reprocessed GOME-2A and GOME-2B vertical ozone profiles products.

3.References

Antón, M., Loyola, D., López, M., et al.: Comparison of GOME-2/MetOpA total ozone data with Brewer spectroradiometer data over the Iberian Peninsula, Annales Geophysicae, 27, 1377–1386, DOI:10.5194/angeo-27-1377-2009, 2009.

Balis, D., Kroon, M., Koukouli, M. E., et al.: Validation of Ozone Monitoring Instrument total ozone column measurements using Brewer and Dobson spectrophotometer ground-based observations, J. Geophys. Res., 112, D24S46, doi:10.1029/2007JD008796, 2007a

Balis, D., Lambert, J.-C., Van Roozendael, M., Spurr, R., Loyola, D., Livschitz, Y., Valks, P., Amiridis, V., Gerard, P., Granville, J., Zehner, C.: Ten years of GOME/ERS2 total ozone data—The new GOME data processor (GDP) version 4: 2. Ground-based validation and comparisons with TOMS V7/V8, J. Geophys. Res., 112, D07307, doi:10.1029/2005JD006376, 2007b

Boyd, I. S., A. D. Parrish, L. Froidevaux, T. von Clarmann, E. Kyrölä, J. M. Russell III, and J. M. Zawodny (2007), Ground-based microwave ozone radiometer measurements compared with Aura-MLS v2.2 and other instruments at two Network for Detection of Atmospheric Composition Change sites, J. Geophys. Res., 112, D24S33, doi:10.1029/2007JD008720.

Brewer, A. and J. Milford, The Oxford Kew ozone sonde, Proc. Roy. Soc. London, Ser. A, 256, 470, 1960.

Delcloo A., and L. Kins (2009, 2012): O3M SAF Validation report on GOME-2 near real-time and offline ozone profiles.

Delcloo A. and K. Kreher (2013): O3M SAF Validation report on GOME-2 near real-time and offline ozone profiles.

Delcloo A. (2020): AC SAF Validation report on GOME-2 near real-time and offline global tropospheric ozone

Garane, K., Lerot, C., Coldewey-Egbers, M., Verhoelst, T., Koukouli, M. E., Zyrichidou, I., Balis, D. S., Danckaert, T., Goutail, F., Granville, J., Hubert, D., Keppens, A., Lambert, J.-C., Loyola, D., Pommereau, J.-P., Van Roozendael, M., and Zehner, C.: Quality assessment of the Ozone_cci Climate Research Data Package (release 2017) – Part 1: Ground-based validation of total ozone column data products, Atmos. Meas. Tech., 11, 1385–1402, https://doi.org/10.5194/amt-11-1385-2018, 2018.

Garane, K., Koukouli, M.-E., Verhoelst, T., Lerot, C., Heue, K.-P., Fioletov, V., Balis, D., Bais, A., Bazureau, A., Dehn, A., Goutail, F., Granville, J., Griffin, D., Hubert, D., Keppens, A., Lambert, J.-C., Loyola, D., McLinden, C., Pazmino, A., Pommereau, J.-P., Redondas, A., Romahn, F., Valks, P., Van Roozendael, M., Xu, J., Zehner, C., Zerefos, C., and Zimmer, W.: TROPOMI/S5P total ozone column data: global ground-based validation and consistency with other satellite missions, Atmos. Meas. Tech., 12, 5263–5287, https://doi.org/10.5194/amt-12-5263-2019, 2019.

Garane, K., Koukouli, M. E., D. Balis, K.P. Heue, D. Loyola: GOME-2/MetOpC GDP 4.9 total ozone data validation, Validation Report SAF/AC/AUTH/VR/O3, Issue 1/2020, https://acsaf.org/docs/vr/Validation_Report_NTO_OTO_O3_May_2020.pdf, (last access: 22 April 2021), 2020

García, O. E., Sanromá, E., Schneider, M., Hase, F., León-Luis, S. F., Blumenstock, T., Sepúlveda, E., Redondas, A., Carreño, V., Torres, C., and Prats, N.: Improved ozone monitoring by ground-based FTIR spectrometry, Atmos. Meas. Tech., 15, 2557–2577, https://doi.org/10.5194/amt-15-2557-2022, 2022

Godin S., G. Megie, J. Pelon: Systematic lidar measurements of the stratospheric ozone vertical distribution, GRL, 16, 6, doi/10.1029/GL016i006p00547, 1998

Hao, N., Koukouli, M. E., Inness, A., Valks, P., Loyola, D. G., Zimmer, W., Balis, D. S., Zyrichidou, I., Van Roozendael, M., Lerot, C., and Spurr, R. J. D.: GOME-2 total ozone columns from MetOp-A/MetOp-B and assimilation in the MACC system, Atmos. Meas. Tech., 7, 2937-2951, https://doi.org/10.5194/amt-7-2937-2014, 2014

Hovila, D., S. Hassinen, P. Valks, J., S. Kiemle, O. Tuinder, H. Joench-Soerensen, Product Requirements Document, Issue 1.5, SAF/AC/FMI/RQ/PRD/001, Issue 1.5, June 2019

Hocke, K., Kämpfer, N., Ruffieux, D., Froidevaux, L., Parrish, A., Boyd, I., von Clarmann, T., Steck, T., Timofeyev, Y. M., Polyakov, A. V., and Kyrölä, E.: Comparison and synergy of stratospheric ozone measurements by satellite limb sounders and the ground-based microwave radiometer SOMORA, Atmos. Chem. Phys., 7, 4117–4131, https://doi.org/10.5194/acp-7-4117-2007, 2007.

Keckhut, Philippe, et al. "Review of ozone and temperature lidar validations performed within the framework of the Network for the Detection of Stratospheric Change." Journal of Environmental Monitoring 6.9 (2004): 721-733, https://doi.org/10.1029/GL016i006p00547.

Keppens, A., Lambert, J.-C., Granville, J., Miles, G., Siddans, R., van Peet, J. C. A., van der A, R. J., Hubert, D., Verhoelst, T., Delcloo, A., Godin-Beekmann, S., Kivi, R., Stübi, R., and Zehner, C.: Round-robin evaluation of nadir ozone profile retrievals: methodology and application to MetOp-A GOME-2, Atmos. Meas. Tech., 8, 2093–2120, https://doi.org/10.5194/amt-8-2093-2015, 2015.

Kobayashi, J., and Y. Toyama, On various methods of measuring the vertical distribution of atmospheric ozone (III) - Carbon iodine type chemical ozone sonde-. Pap. Met. Geophys., 17, 113-126, 1966

Komhyr, W.D., Electrochemical concentration cells for gas analysis, Ann. Geoph., 25, 203-210, 1969.

Komhyr, W.D., Development of an ECC-Ozonesonde, NOAA Techn. Rep. ERL 200-APCL 18ARL-149, 1971.

Koukouli, M. E., Balis, D. S., Loyola, D., Valks, P., Zimmer, W., Hao, N., Lambert, J.-C., Van Roozendael, M., Lerot, C., and Spurr, R. J. D.: Geophysical validation and long-term consistency between GOME-2/MetOp-A total ozone column and measurements from the sensors GOME/ERS-2, SCIAMACHY/ENVISAT and OMI/Aura, Atmos. Meas. Tech., 5, 2169-2181, https://doi.org/10.5194/amt-5-2169-2012, 2012.

Koukouli, M. E., Lerot, C., Granville, J., Goutail, F., Lambert, J.-C., Pommereau, J.-P., Balis, D., Zyrichidou, I., Van Roozendael, M., Coldewey-Egbers, M., Loyola, D., Labow, G., Frith, S., Spurr, R., and Zehner, C.: Evaluating a new homogeneous total ozone climate data record from GOME/ERS-2, SCIAMACHY/Envisat, and GOME-2/MetOp-A, J. Geophys. Res., 120, 12296–12312, https://doi.org/10.1002/2015JD023699, 2015

Koukouli, M. E., Zyrichidou, I., Balis, D. S., Valks, P., Hao, N., and Valks, P.: GOME-2/MetOpA & GOME-2/MetOpB GDP 4.8 total ozone data validation, Validation Report SAF/O3M/AUTH/VRR/O3, Issue 1/0, available at: https://acsaf.org/docs/vr/Validation_Report_NTO_OTO_DR_O3_GDP48_Dec_2015.pdf (last access: 22 April 2021), 2015

Leblanc, T., and I. S. McDermid, Stratospheric Ozone Climatology From Lidar Measurements at Table Mountain (34.4°N, 117.7°W) and Mauna Loa (19.5°N, 155.6°W), J. Geophysical Research, 105, 14,613-14,623, 2000.

Lee, G. Mégie, H. Nakane and R. Neuber, Review of ozone and temperature lidar validations performed within the framework of the Network for the Detection of Stratospheric Change, J. Environ. Monit., 6, 721 – 733, doi:10.1039/B404256E, 2004.

Lobsiger E., K.F. Künzi and H.U. Dütsch, Comparison of stratospheric ozone profiles retreived from microwave-radiometer and Dobson-spectrometer data, J. Atm. and Terr. Phys., 46, 799-806, 1984.

Loyola, D., Koukouli, M., Valks, P., Balis, D., Hao, N., Van Roozendael, M., Spurr, R., Zimmer, W., Kiemle, S., Lerot, C., and Lambert, J-C.: The GOME-2 Total Column Ozone Product: Retrieval Algorithm and Ground-Based Validation, J. Geophys. Res., 116, D07302, doi:10.1029/2010JD014675, 2011.

Parrish, A., R.L. de Zafra, P.M. Solomon, and J.W. Barrett, A ground-based technique for millimeter wave spectroscopic observations of stratospheric trace constituents, Radio Sci., 23, 106-118, 1988.

Rodgers C.D., Characterization and Error Analysis of Profiles Retrieved from Remote Sounding Measurements, J. Geophys. Res., 95, 5587-5595, 1990.

Sterling, C. W., Johnson, B. J., Oltmans, S. J., Smit, H. G. J., Jordan, A. F., Cullis, P. D., Hall, E. G., Thompson, A. M., and Witte, J. C.: Homogenizing and estimating the uncertainty in NOAA's long-term vertical ozone profile records measured with the electrochemical concentration cell ozonesonde, Atmos. Meas. Tech., 11, 3661–3687, https://doi.org/10.5194/amt-11-3661-2018, 2018.

Steinbrecht W., et al. (2006), Long-term evolution of upper stratospheric ozone at selected stations of the Network for the Detection of Stratospheric Change (NDSC), J. Geophys. Res., 111, D10308, doi:10.1029/2005J

Thompson, A. M., Witte, J. C., Sterling, C., Jordan, A., Johnson, B. J., Oltmans, S. J., … Thiongo, K. (2017). First reprocessing of Southern Hemisphere Additional Ozonesondes (SHADOZ) ozone profiles (1998–2016): 2. Comparisons with satellites and ground-based instruments. Journal of Geophysical Research: Atmospheres, 122. https://doi.org/10.1002/2017JD027406.

Tuinder, O., van Oss, R., de Haan, J. and Delcloo, A. (2022). ATBD of the Vertical Ozone Profile algorithm, ACSAF/KNMI/ATBD/001, Issue 2.1.3, November 2022.

Tuinder, O. (2022) Product User Manual (PUM) of the Vertical Ozone Profile Products, ACSAF/KNMI/PUM/001, Issue 2.5.2, November 2022.

APPENDIX I

Table A. 1: List of Dobson ground-based stations used for the comparisons

ST. ID	NAME	COUNTRY	LONG.	LAT.	Last day of available measurements	
			degrees	Degrees	Collocated to GOME-2A	Collocated to GOME-2B & 2C
2	Tamanrasset	Algeria	5.52	22.78	15-NOV-2021	31-AUG-2022
10	New Delhi	India	77.18	28.63	15-NOV-2021	31-AUG-2022
11	Quetta	Pakistan	66.95	30.19	31-DEC-2020	31-DEC-2020
12	Sapporo	Japan	141.33	43.06	31-JAN-2018	31-JAN-2018
14	Tateno	Japan	140.13	36.05	11-NOV-2021	31-AUG-2022
19	Bismarck	USA	-100.75	46.77	05-NOV-2021	30-AUG-2022
20	Caribou	USA	-68.01	46.87	31-JUL-2018	31-JUL-2018
27	Brisbane	Australia	153.08	-27.42	11-NOV-2021	31-AUG-2022
29	Macquarie island	Australia	158.94	-54.50	14-NOV-2021	31-AUG-2022
31	Mauna_loa	USA	-155.58	19.54	14-NOV-2021	31-AUG-2022
35	Arosa	Switzerland	9.67	46.78	05-NOV-2013	07-NOV-2013
40	Haute Province	France	5.75	43.92	15-NOV-2021	30-JUN-2022
43	Lerwick	UK	-1.18	60.13	15-NOV-2021	31-AUG-2022
51	Reykjavik	Iceland	-21.90	64.13	13-NOV-2021	31-AUG-2022
53	Uccle	Belgium	4.36	50.80	29-MAY-2009	
57	Halley Bay	Antarctica	-26.18	-75.62	30-SEP-2020	30-SEP-2020
67	Boulder	USA	-105.26	39.99	14-NOV-2021	31-AUG-2022
68	Belsk	Poland	20.79	51.84	15-NOV-2021	31-AUG-2022
82	Lisbon	Portugal	-9.13	38.77	12-NOV-2021	31-AUG-2022
84	Darwin	Australia	130.88	-12.42	12-NOV-2021	31-AUG-2022
91	Buenos Aires	Argentina	-58.48	-34.59	31-MAR-2019	31-MAR-2019
96	Hradec_kralove	Czech Rep.	15.84	50.18	15-NOV-2021	30-AUG-2022
99	Hohenpeissenberg	Germany	11.01	47.80	11-NOV-2021	30-AUG-2022
101	Syowa	Antarctica	39.58	-69.00	15-NOV-2021	31-JAN-2022
105	Fairbanks	USA	-147.87	64.82	28-OCT-2021	31-MAY-2022
106	Nashville	USA	-86.57	36.25	31-JUL-2017	03-JUL-2017
107	Wallops island	USA	-75.46	37.94	10-NOV-2021	10-AUG-2022
111	Amundsen-Scott	Antarctica	-24.80	-90.00	26-FEB-2013	31-DEC-2021
152	Cairo	Egypt	31.28	30.08	31-OCT-2021	31-OCT-2021
159	Perth	Australia	115.97	-31.92	02-JUL-2016	02-JUL-2016
175	Nairobi	Kenya	36.75	-1.30	24-DEC-2012	31-DEC-2012

190	Naha	Japan	127.68	26.20	29-JAN-2018	31-JAN-2018
191	Samoa	USA	-170.56	-14.25	08-NOV-2021	30-AUG-2022
199	Barrow	USA	-156.61	71.32	23-AUG-2021	24-AUG-2022
200	Cachoeira-Paulista	Brazil	-46.20	-23.50	28-NOV-2018	28-NOV-2018
208	Shiangher	China	116.96	39.75	13-NOV-2021	31-AUG-2022
209	Kunming	China	102.21	25.03	30-DEC-2014	30-DEC-2014
213	El Arenosillo	Spain	-6.73	37.10	21-DEC-2018	21-DEC-2018
214	Singapore	Singapore	103.87	1.32	23-JUL-2012	
216	Bangkok	Thailand	100.62	13.67	15-NOV-2021	31-AUG-2022
219	Natal	Brazil	-35.20	-6.00	23-SEP-2020	31-AUG-2022
226	Bucharest	Romania	26.13	44.48	12-NOV-2021	22-AUG-2022
232	Vernadsky-Faraday	Antarctica	-64.26	-65.25	15-AUG-2017	17-AUG-2017
245	Aswan	Egypt	32.78	23.97	16-AUG-2021	18-AUG-2021
252	Seoul	Korea	126.95	37.57	14-NOV-2021	31-AUG-2022
253	Melbourne	Australia	144.83	-37.67	14-NOV-2021	16-AUG-2022
256	Lauder	N. Zealand	169.68	-45.04	14-NOV-2021	25-JUL-2022
265	Irene	S. Africa	28.22	-25.91	13-NOV-2021	27-AUG-2022
268	Arrival Heights	Antarctica	166.66	-77.83	11-NOV-2021	13-MAR-2022
284	Vindeln	Sweden	19.77	64.23	19-OCT-2021	31-AUG-2022
293	Athens	Greece	23.73	37.98	30-SEP-2019	30-SEP-2019
311	Havana	Cuba	-82.35	23.15	08-AUG-2015	08-DEC-2015
339	Ushuaia	Argentina	-68.31	-54.85	30-DEC-2018	31-DEC-2018
340	Springbok	S. Africa	17.90	-29.67	15-NOV-2021	28-AUG-2022
341	Hanford	USA	-119.63	36.32	06-NOV-2021	09-FEB-2022
342	Comodoro Rivadavia	Argentina	-67.50	-45.78	14-FEB-2019	14-FEB-2019
343	Salto	Uruguay	-57.95	-31.38	28-FEB-2013	28-FEB-2013
409	Hurghada	EGU	33.75	27.42	15-NOV-2021	30-DEC-2021
410	Amberd	ARM	44.25	40.38	13-NOV-2021	31-AUG-2022

Table A. 2: List of Brewer ground-based stations used for the comparisons [updated]

ST. ID	NAME	COUNTRY	LONG.	LAT.	Last day of available measurements	
			degrees	degrees	Collocated to GOME-2A	Collocated to GOME-2B & 2C
2	Tamanrasset	Algeria	5.52	22.78	30-SEP-2017	30-SEP-2017
12	Sapporo	Japan	141.33	43.06	14-NOV-2021	31-JAN-2022
14	Tateno	Japan	140.13	36.05	11-NOV-2021	31-AUG-2022
21	Edmonton	Canada	-114.1	53.55	14-NOV-2021	31-AUG-2022
24	Resolute	Canada	-94.98	74.72	04-OCT-2021	31-AUG-2022
35	Arosa	Switzerland	9.67	46.78	31-DEC-2013	31-DEC-2013
53	Uccle	Belgium	4.36	50.8	15-NOV-2021	31-AUG-2022
65	Toronto	Canada	-79.47	43.78	14-NOV-2021	31-AUG-2022
76	Goose	Canada	-60.39	53.29	14-NOV-2021	31-AUG-2022
77	Churchill	Canada	-93.82	58.74	10-NOV-2021	31-AUG-2022
89	Ny_alesund	Norway	11.92	78.92	30-JUN-2021	30-JUN-2021
95	Taipei	Taiwan	121.48	25.02	13-NOV-2021	31-AUG-2022
96	Hradec Kralove	Czech Republic	15.84	50.18	15-NOV-2021	31-AUG-2022
99	Hohenpeissenberg	Germany	11.01	47.8	11-NOV-2021	30-AUG-2022
100	Budapest	Hungary	19.18	47.43	28-DEC-2013	28-DEC-2013
174	Lindenberg	Germany	14.12	52.22	31-JAN-2014	31-JAN-2014
190	Naha	Japan	127.68	26.2	14-NOV-2021	30-JAN-2022
213	El Arenosillo	Spain	-6.73	37.1	13-NOV-2021	31-AUG-2022
261	Thessaloniki	Greece	22.96	40.63	13-NOV-2021	31-AUG-2022
262	Sodankyla	Finland	26.63	67.36	31-MAY-2010	
267	Sondrestrom	Greenland	-50.95	66.99	31-AUG-2017	31-AUG-2017
279	Norkoping	Sweden	16.15	58.58	15-NOV-2021	31-AUG-2022
282	Kislovodsk	Russia	42.66	43.73	31-MAR-2020	31-MAR-2020
284	Vindeln	Sweden	19.77	64.23	14-NOV-2021	31-AUG-2022
290	Saturna	Canada	-123.13	48.78	14-NOV-2021	31-AUG-2022
295	Mt. Waliguan	China	100.9	36.29	15-NOV-2021	28-FEB-2022
305	Rome University	Italy	12.52	41.9	26-DEC-2017	29-DEC-2017
308	Madrid	Spain	-3.72	40.45	14-NOV-2021	31-AUG-2022
315	Eureka	Canada	-86.42	80.05	25-SEP-2021	31-AUG-2022
316	Debilt	Netherlands	5.18	52.1	30-SEP-2021	30-SEP-2021
318	Valentia	Ireland	-10.25	51.94	15-NOV-2021	31-AUG-2022
322	Petaling Jaya	Malaysia	101.65	3.1	31-MAR-2019	30-MAR-2019
326	Longfenshan	China	127.6	44.73	13-NOV-2021	30-MAR-2022

330	Hanoi	Vietnam	105.8	21.2	15-NOV-2021	31-AUG-2022
331	Poprad-Ganovce	Slovakia	20.32	49.03	13-NOV-2021	31-AUG-2022
346	Murcia	Spain	-1.17	38	14-NOV-2021	31-AUG-2022
348	Ankara	Turkey	32.88	39.95	31-DEC-2015	31-DEC-2015
352	Manchester	GBR	-2.23	53.47	13-NOV-2021	31-AUG-2022
353	Reading	GBR	-0.94	51.44	14-NOV-2021	31-AUG-2022
376	Mrsa Mtrouh	Egypt	27.22	31.33	31-OCT-2020	31-OCT-2020
401	Santa Cruz	Spain	-16.25	28.47	15-NOV-2021	31-AUG-2022
405	La Coruna	Spain	-8.47	43.33	13-NOV-2021	31-AUG-2022
411	Zaragoza	Spain	-0.91	41.63	14-NOV-2021	31-AUG-2022
435	Paramaribo	SUR	-55.21	5.81	12-SEP-2021	16-SEP-2021
447	Goddard	USA	-76.83	38.99	20-SEP-2010	
456	Care	Canada	-79.78	44.23	06-MAR-2021	08-MAR-2021
468	Cape d'aguilar	HKG	114.26	22.21	30-DEC-2010	
476	Andoya	NOR	16.01	69.28	09-OCT-2020	09-OCT-2020
479	Aosta	Italy	7.36	45.74	15-NOV-2021	31-AUG-2022
481	Tomsk	Russia	85.1	56.5	26-JUN-2012	
512	Univ._of_Toronto	Canada	-79.4	43.66	13-MAR-2012	

Table A. 3 List of all ozonesonde stations used for the comparisons

Station	Lat	long	nr of profiles	Last day measure-ment
ALAJUELA	9.98	-84.21	466	14-DEC-18
ALERT	82.5	-62.33	441	05-DEC-18
ASCENSION	-7.98	-14.42	260	19-DEC-18
BRATTS_LAKE	50.2	-104.7	218	28-SEP-11
BROADMEADOWS	-37.69	144.95	567	19-DEC-18
CHURCHIL	58.74	-94.07	203	12-MAR-14
DAVIS	-68.577	77.973	207	27-NOV-13
DEBILT	52.1	5.18	608	27-DEC-18
EDMONTON	53.55	-114.1	264	09-APR-14
EGBERT	44.23	-79.78	211	31-AUG-11
EUREKA	80	-85.56	442	01-OCT-14
FIJI	-18.1	178.4	174	30-DEC-18
GOOSE_BAY	53.3	-60.36	271	17-JAN-13
HILO	19.717	-155.083	517	26-DEC-18
HOHENPEISSENBERG	47.8	11.02	1431	28-DEC-18
IRENE	-25.9	28.22	130	07-NOV-18
JAVA	-7.5	112.6	90	30-OCT-13
KELOWNA	49.67	-119.4	291	09-APR-14
KUALA_LUMPUR	2.73	101.7	252	21-DEC-18
LAUDER	-45.045	169.684	559	23-DEC-18
LA_REUNION	-20.99	55.48	250	22-JAN-18
LERWICK	60.14	-1.19	580	26-DEC-18
MACQUARIE_ISL	-54.5	158.94	542	25-DEC-18
NAHA	26.2	127.683	401	30-JAN-18
NAIROBI	-1.27	36.8	482	19-DEC-18
NATAL	-5.42	-35.38	313	11-DEC-18
NEUMAYER	-70.39	-8.15	822	26-DEC-18
NY-ALESUND	78.93	11.95	881	28-DEC-18
PARAMARIBO	5.81	-55.21	363	31-DEC-18
PAYERNE	46.817	6.95	1621	27-DEC-18
RESOLUTE	74.71	-94.97	226	02-APR-14
SAMOA	-14.23	-170.56	369	19-DEC-18
SAN_CRISTOBAL	-0.92	-89.6	119	07-JAN-16
SAPPORO	43.06	141.3315	462	29-JAN-18
SODANKYLA	67.3666	26.6297	638	20-DEC-18
SOUTH_POLE	-89.99	-24.8	168	30-DEC-18
TATENO-TSUKUBA	36.1	140.1	532	26-DEC-18
TORONTO	43.78	-79.47	207	26-DEC-12
UCCLE	50.8	4.35	1689	28-DEC-18
USHUAIA	-54.85	-68.308	158	26-OCT-16
VALENTIA	51.93	-10.25	290	28-DEC-18
WALLOPS_ISL	37.84	-75.48	476	19-JUL-16
YARMOUTH	43.87	-66.11	286	02-APR-14

Table A. 4: List of all lidar, MWR and FTIR stations used for the comparisons

STATION	Latitude	Longitude	No. of profiles	Last measurement used here
Lidar:				
HOHENPEISSENBERG, Germany	47.8	11.02	1035	31-AUG-2022
OBS. HAUTE PROVENCE, France	43.94	5,71	1048	31-AUG-2022
TABLE MOUNTAIN, Ca., USA	34.4	117.7	949	31-AUG-2022
MAUNA LOA, Hawaii, USA	19.54	155.58	1052	31-AUG-2022
LAUDER, New Zealand	-45.04	169.68	247	30-JUL-2021
Microwave:				
NY-ALESUND, Spitzbergen, Norway	78.93	11.95	23432	30-JUL-2021
BERN, Switzerland	46.95	7.45	18509	31-AUG-2022
PAYERNE, Switzerland	46.82	6.95	7078	31-AUG-2022
MAUNALOA, Hawaii, USA	19.54	155.58	1888	31-AUG-2022
LAUDER, New Zealand	-45.04	169.68	437	31-AUG-2016
FTIR:				
NY-ALESUND, Spitzbergen, Norway	78.93	11.95	402	31-AUG-2022
HOHENPEISSENBERG, Germany	47.8	11.02	7657	31-AUG-2022
MAUNALOA, Hawaii, USA	19.54	155.58	4967	31-AUG-2022
IZANA, Tenerife, Spain	28.3	16.5	152	31-AUG-2022
EUREKA, Canada	80.05	86.42	3842	31-AUG-2022
KIRUNA, Sweden	67.84	20.41	345	31-AUG-2022
REUNION-MAIDO, France	21.1	55.4	389	31-AUG-2022
Thule, Greenland	76.53	68.74	773	31-AUG-2022
LAUDER, New Zealand	-45.04	169.68	7917	31-AUG-2022